

TECHNICAL UNIVERSITY OF CRETE
SCHOOL OF MINERAL RESOURCES ENGINEERING
MSc PETROLEUM ENGINEERING

Master Thesis

“LARGE-SCALE FULL-TIME FIELD GAS LIFT DESIGN”

Author

Nanidou Konstantina

Examination Committee:

1. Prof. Varotsis Nikolaos (Supervisor)
2. Prof. Pasadakis Nikolaos
3. Prof. Gaganis Vassilios

*A thesis submitted in fulfillment of the requirements for the
Master degree of Petroleum Engineering
in the
School of Mineral Resources Engineering
Technical University of Crete*

Chania, 2018

*The MSc Program in Petroleum Engineering of the Technical University of Crete,
was attended and completed by Mrs. Nanidou Konstantina,
due to the Hellenic Petroleum Group Scholarship award.*

Table of Contents

List of Figures	v
List of Tables	vii
Acknowledgements	ix
Abstract	x
1. Introduction	1
1.1 Importance of petroleum	1
1.2 Extraction of petroleum.....	1
1.3 Artificial lift.....	2
1.4 PIPESIM.....	2
1.5 tNavigator Black oil Simulator	3
2. Well Performance- Deliverability.....	4
2.1 Natural Drive mechanisms	4
2.2 Nodal Analysis	6
2.3 Tubing Performance of a Well.....	8
2.4 Gradient Curves.....	8
2.5 Pressure Traverse Curves	9
3. Artificial Lift Methods	10
3.1 Pump Systems	10
3.2 Gas Lift.....	10
3.3 Gas lift equipment	12
3.3.1 Gas lift Advantages.....	13
3.3.2 Gas Lift Disadvantages	13
4. Description of the Reservoir Model.....	14
4.1 Fluid properties	15
4.2 Deviation Survey of the Wells	16
4.3 Evaluation of wells' deliverability	23
4.3.1 Worst-case scenario	25
5. Gas Lift Design.....	27
5.1 Tubing Size Optimization	27

5.1.1	Analysis for the tubing selection.....	28
5.1.2	Input Data for the Gas Lift.....	29
5.1.3	Tubing Selection Methodology.....	31
5.1.4	Conclusion	33
5.1.5	Evaluation of the Gas lift design.....	34
5.1.6	Gas lift design equipment for well W3	35
6.	Results of the Gas lift design	37
7.	Conclusion	42
	Bibliography	43
8.	APPENDIX.....	44

List of Figures

<i>Figure 2.1 Natural drive mechanisms occur in the reservoir</i>	5
<i>Figure 2.2 System analysis illustration (Kermit E. Brown, James F. Lea, 1985)</i>	7
<i>Figure 3.1 Simple Gas Lift Schematic (Deni et al, 2007)</i>	11
<i>Figure 3.2 Gas injection valve</i>	12
<i>Figure 3.3 Artificial Gas lift system</i>	13
<i>Figure 4.1 3D Map of the pressures of the Reservoir model (tNavigator, v4.1.3, 2015)</i>	14
<i>Figure 4.2 Relative Permeabilities Curves Water-Oil (tNavigator, v4.1.3, 2015)</i>	16
<i>Figure 4.3 Design of slant well type (Mitchell, 2011)</i>	17
<i>Figure 4.4 Deviation survey W3 (PIPESIM Steady-State Multiphase Flow Simulator)</i>	20
<i>Figure 4.5 Deviation survey W22 (PIPESIM Steady-State Multiphase Flow Simulator)</i>	21
<i>Figure 4.6 Deviation survey W27 (PIPESIM Steady-State Multiphase Flow Simulator)</i>	21
<i>Figure 4.7 Deviation survey W31 (PIPESIM Steady-State Multiphase Flow Simulator)</i>	21
<i>Figure 4.8 Deviation survey W33 (PIPESIM Steady-State Multiphase Flow Simulator)</i>	22
<i>Figure 4.9 Deviation survey W35 (PIPESIM Steady-State Multiphase Flow Simulator)</i>	22
<i>Figure 4.10 Deviation survey W40 (PIPESIM Steady-State Multiphase Flow Simulator)</i>	22
<i>Figure 4.11 Deviation survey W48 (PIPESIM Steady-State Multiphase Flow Simulator)</i>	23
<i>Figure 4.12 Deviation survey W50 (PIPESIM Steady-State Multiphase Flow Simulator)</i>	23
<i>Figure 4.13 Pressure Traverse plot for well W3 (PIPESIM Steady-State Multiphase Flow Simulator, 2017)</i>	24
<i>Figure 5.1 Pressure Traverse plot for the well W3 (PIPESIM Steady-State Multiphase Flow Simulator)</i>	29
<i>Figure 5.2 Total Gas production of the Field</i>	31
<i>Figure 5.3 Liquid flowrate for different tubing sizes (well W3)</i>	33
<i>Figure 5.4 Pressure Traverse Plot after the Gas Lift installation (PIPESIM Steady-State Multiphase Flow Simulator)</i>	34
<i>Figure 5.5 Artificial Gas Lift equipment (PIPESIM Steady-State Multiphase Flow Simulator, 2017)</i>	35
<i>Figure 5.6 Gas Lift visualization for the Well W3 (PIPESIM Steady-State Multiphase Flow Simulator, 2017)</i>	35
<i>Figure 5.7 Pressure vs Depth of the Gas Lift installation (PIPESIM Steady-State Multiphase Flow Simulator, 2017)</i>	36
<i>Figure 8.1 Artificial lift configuration for well W3</i>	44
<i>Figure 8.2 Artificial lift configuration for well W22</i>	44
<i>Figure 8.3 Artificial lift configuration for well W31</i>	45
<i>Figure 8.4 Artificial lift configuration for well W33</i>	45

List of Figures

Figure 8.5 Artificial lift configuration for well W48 46
Figure 8.6 Artificial lift configuration for well W50 46
Figure 8.7 Artificial lift equipment W22..... 47
Figure 8.8 Artificial lift equipment W31..... 47
Figure 8.9 Artificial lift equipment W33..... 47
Figure 8.10 Artificial lift equipment W35..... 47
Figure 8.11 Artificial lift equipment W48..... 47
Figure 8.12 Artificial lift equipment W50..... 48
Figure 8.13 Pressure Traverse Curve after Gas Lift installation for well W22 48
Figure 8.14 Pressure Traverse Curve after Gas Lift installation for well W31 48
Figure 8.15 Pressure Traverse Curve after Gas Lift installation for well W33 49
Figure 8.16 Pressure Traverse Curve after Gas Lift installation for well W48..... 49
Figure 8.17 Pressure Traverse Curve after Gas Lift installation for well W50..... 50

List of Tables

<i>Table 4:1 Horizontal distances of the wells from the rig</i>	15
<i>Table 4:2 Properties of the fluid</i>	15
<i>Table 4:3 MD and TVD of the wells</i>	19
<i>Table 4:4 MD and TVD of the wells</i>	20
<i>Table 4:5 Results of Pressure Traverse curves for the wells</i>	25
<i>Table 4:6 Worst case scenarios of the wells</i>	26
<i>Table 4:7 Results of Pressure Traverse curves for the worst-case scenarios</i>	26
<i>Table 5:1 Liquid flowrates prediction</i>	28
<i>Table 5:2 Well Data for W3</i>	29
<i>Table 5:3 Fluid properties for W3</i>	29
<i>Table 5:4 Reservoir Data for W3</i>	30
<i>Table 5:5 Gas Lift Design Data for W3</i>	30
<i>Table 5:6 Gas lift of W3, tubing ID= 2.441in</i>	32
<i>Table 5:7 Gas lift of W3, tubing ID= 2.75in</i>	32
<i>Table 5:8 Gas lift of W3, tubing ID= 3.5in</i>	32
<i>Table 5:9 Gas lift of W3, tubing ID= 4in</i>	32
<i>Table 5:10 Gas lift of W3, tubing ID= 5in</i>	33
<i>Table 6:1 Gas lift results for well W3</i>	37
<i>Table 6:2 Gas lift results for well W22</i>	37
<i>Table 6:3 Gas lift results for well W31</i>	38
<i>Table 6:4 Gas lift results for well W33</i>	38
<i>Table 6:5 Gas lift results for well W35</i>	39
<i>Table 6:6 Gas lift results for well W48</i>	39
<i>Table 6:7 Gas lift results for well W50</i>	40
<i>Table 6:8 Deviation between the predicted and calculated production</i>	40

List of Tables

Acknowledgements

Firstly, I would like to express my gratitude to my supervisor Professor Vasilis Gaganis for his guidance and the scientific comments during this thesis. I would also like to thank Professor Nikolaos Varotsis for being part of my thesis committee.

Further, I would like to express my sincere appreciation to Professor Nikolaos Pasadakis, who believed in me from the beginning of our cooperation, and gave me the opportunity to work with him.

Above all, I would like to thank to my family for supporting me during my life and stimulating me to follow my dreams. I am eternally grateful to my parents, who were always backing me up emotionally and financially all these difficult and stressful years.

Last but not least, some special words of gratitude go to all of my friends for those memories that we have shared together, which no matter how far we are, will always follow and define us.

Thank you all,

Nanidou Konstantina.

Abstract

Nodal analysis is the standard tool to use when designing a wellbore provided that steady state flow conditions prevail in the well. However, when operating conditions such as GOR, water cut, bottomhole flowing pressure or rate vary over time nodal analysis cannot be used directly. As a result, it cannot be directly applied to the bottom hole conditions which are obtained from a reservoir simulation program. To design a well under such transient reservoir conditions, pressure traverse curves need to be combined to the well flow data.

In this thesis a dynamic reservoir model was set up and history matched by using the tNavigator reservoir simulation software. Firstly, the deviation survey of each well was needed to be designed in order to meet their location in the reservoir space. Subsequently, well flow data which is required to design the appropriate wellbore were exported and further utilized as input for the PIPESIM well flow simulator, and each well was checked for its ability to bear the prediction at the surface without the need for artificial lift.

For each well in the reservoir model that needed a gas lift, such a system was designed to compensate the required production rates while respecting the available bottom hole pressure, as indicated by the reservoir simulation scenario. The gas lift system design consisted of selecting the appropriate well tubing size, the number and depth of injection valves, the gas injection pressure and the injected gas flowrate.

Additionally, an evaluation of the well performance was run to test if the reservoir simulation schedule is running with no production problems.

1. Introduction

1.1 Importance of petroleum

Even though nowadays renewable sources of energy are coming into play and are significantly trying to compensate the need for fossil fuels, the majority of modern society energy supply is still provided from fossil fuels. Crude oil is definitely one of the most widely used fossil fuel. Its use ranges from transportation, heating and lighting, petro-chemical industry, power generation and much more. And it would be definitely hard or even impossible to imagine day-to-day life of a man without oil.

1.2 Extraction of petroleum

Despite the widely believed myth that petroleum is accumulated in underground lakes waiting for us to find it, the truth is quite more complicated. Before we come to production of petroleum a long and exhausting exploratory process precedes in which the main role is taken by geologists and geophysicists. By utilizing established methods and their expertise they are able to investigate deep underground geological structures that are likely to be good “candidates” of possible oil reservoirs. Drilling comes into play after the completion of the exploration phase. In this phase by utilization of specific configurations called rigs a well is created, by drilling a deep hole into the earth until connection is established from a possible reservoir to the surface. Steel pipes (casing strings) are introduced into the wellbore in order to prevent collapse, followed by the tubing which prepares the well for the production stage. As a part of completion, perforations (small holes) are penetrated at the bottom of the well in order to establish connection between the well and the reservoir zone and enable the fluid flow to the surface. Finally, a set of valves widely known in industry as “Christmas Tree” is placed at the top, by means of which pressures and flowrate are regulated.

1.Introduction

1.3 Artificial lift

The majority of reservoirs at the start of their life are able to produce fluid naturally with the use of their own energy, widely known as primary drive mechanisms. At early stages of reservoir lifetime well bottomhole pressure is often high enough to overcome total pressure loss caused by fluid flow from bottom hole to the surface and hydrostatic pressure of the column itself. This stage of reservoir lifetime is often called primary production.

Once the energy of stemming from the primary drive mechanism starts to decay or when increased water production affects negatively the hydrostatic pressure of the wells, the wells may need some artificial source of energy in order to deliver targeted quantities of fluid. In this case artificial lift methods need to be implemented such as the required bottomhole pressure can be preserved. Actually, artificial lift adds additional energy to the fluid in the well which, accompanied by the reservoir energy allows the well to flow at desired rate. (Schlumberger, Gas Lift Design and Technology, 1999)

1.4 PIPESIM

PIPESIM is a widely used multiphase well flow simulator which enables the engineers to design the flowlines and the pipeline systems including surface equipment (e.g. separators, pumps, compressors, chokes etc.) The fluid properties can be modeled either by black-oil correlations or in a fully compositional way.

PIPESIM offers users the following features;

- Rigorous Modelling of Oil, Gas and Condensate Multiphase flows
- Many multiphase flow modelling options
- Advanced PVT and physical properties prediction
- Efficient and Productive Windows GUI
- Powerful results features: reports & graphs

and allows the following systems to be modelled;

- Production Wells, including flowline and process equipment
- Horizontal Completion
- Surface facilities
- Injection Wells

PIPESIM, is used throughout this MSc thesis for all calculations regarding setting up of a reliable model and building on it a productive continuous gas lift system. (PIPESIM user Manual, 2017)

1.5 tNavigator Black oil Simulator

The tNavigator reservoir simulation software is used throughout this MSc Thesis for running and the dynamic reservoir model exporting the valuable data from that needed to be imported to the PIPESIM. The new reservoir simulator tNavigator developed by the Rock Flow Dynamics (RFD) technologies, is becoming more and more popular recently because of its obvious increase speed and accuracy to compute simulation results. The system has a user-friendly interface which makes it very attractive. According to its developers, the reason why it computes faster the results of complex reservoir models, lies in the fact that it is written in a modern code language compared to the other simulators as well as that it takes advantage of multicore and manycore shared and distributed memory computing systems.

2. Well Performance- Deliverability

When it comes to the performance of a well a large number of variables such as fluid properties, formation properties and reservoir pressure have a big impact and all of them are interconnected. It is actually a combination of factors that influence the productivity of the well, the performance of the flow in the reservoir and the performance of the production string.

2.1 Natural Drive mechanisms

In this chapter we will briefly review how the various basic concepts come together to help us understand various driving forces and their role in fluid production. Reservoir drive mechanisms are often defined as sources of energy available in the reservoir system which are driving the fluids flows inside the porous media and out through the wellbore. Despite of their significant role, it is not necessarily sufficient of lifting the fluids to the surface. The period in which reservoir depletion is mainly due to reservoir drive mechanisms is commonly referred as “primary production”. A wide variety of primary oil recovery drive mechanisms might be encountered:

- Natural water drive
- Gas-cap drive
- Compaction drive
- Solution gas drive
- Gravity Drainage

Natural water drive

In the cases of reservoirs with neighboring aquifers (water bearing zone) a decline in the reservoir pressure caused by production of fluids, can cause initiation of water inflow into the reservoir. Aquifer water in this process acts as the displacing medium, and depending on aquifer type and size it could be a significant natural way of pressure maintenance. Due to its high sweep efficiency, natural water drive yields high overall recovery, often above 50% of OOIP. (Herriot Watt, Reservoir Engineering , 2005)

Gas-cap drive

For reservoirs that are initially saturated, a primary gas cap lies on top of the oil-bearing zone. Due to the compressible nature of gas it is capable of acting as an energy accumulator. High gas compressibility and the extended gas cap size ensure significant accumulation of energy, which can provide a long lasting and efficient field performance. Up to 35% of the original oil in place can be recovered under a gas-cap drive. (Herriot Watt, Reservoir Engineering , 2005)

Compaction drive

This drive mechanism might be triggered during depletion when rock grains are exposed to stress beyond the elasticity limit. It causes re-compaction of relatively deformed or even destroyed rock grains that might have as consequence gradual or abrupt reduction of the reservoir pore volume. (Herriot Watt, Reservoir Engineering , 2005)

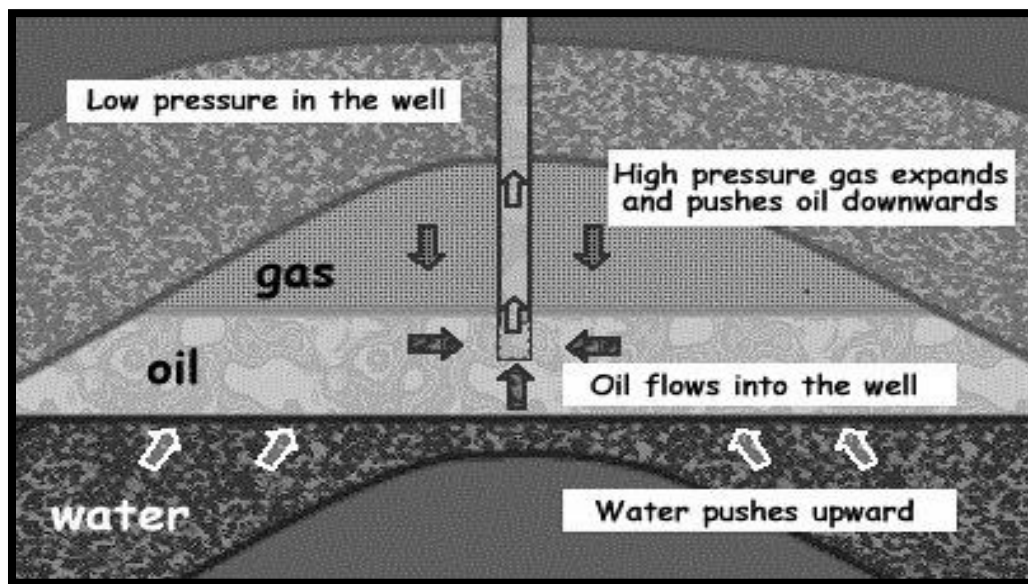


Figure 2.1 Natural drive mechanisms occur in the reservoir

In order to achieve higher field recovery, secondary and tertiary oil recovery methods (usually referred to as Enhanced Oil Recovery methods, EOR) often need to be implemented. (Herriot Watt, Reservoir Engineering , 2005)

2. Well Performance- Deliverability

Solution gas drive

A natural effect of reservoir depletion, is the decay of the reservoir pressure, unless it is maintained either by natural water influx or by using some pressure maintenance technology. If that is not the case reservoir pressure will eventually drop below the bubble point pressure. That has as effect dissolution of gas from the oil phase. The process itself provides energy required for oil phase displacement and as pressure drops further the highly compressible gas expands and enhances the displacing effect. (Herriot Watt, Reservoir Engineering , 2005)

Gravity Drainage

This production drive is considered as a minor contributor to total recovery, but generally associated with later stages of production where its effect can be recognized due to weakening of other drive mechanisms that have been dominant in earlier years of production. Gravity drainage drive is explained as effect of relative density forces of present fluids causing fluids to drain towards the production wells. (Herriot Watt, Reservoir Engineering , 2005)

2.2 Nodal Analysis

For many years Nodal Analysis has been the standard method for analyzing the performance of systems composed of interacting components. Electrical circuits, complex pipeline networks and centrifugal pumping systems are all analyzed using this method. Its application to well producing systems was first proposed by Gilbert in 1954 while Mach, Proano, and Brown in 1979 further developed the concept.

It is often described as the appropriate tool to use to set up a systematic approach to oil and gas wells optimization so as to optimize every component of the system in order to achieve the targeted flow rate.

The standard objectives of this method are to evaluate the flow rate which an existing well can deliver while taking into account its geometry and completion limitations. Moreover, the method is used to determine at which time and under which conditions a well could possibly load or die. or to select the most cost-effective moment for installation of artificial lift and the appropriate

2. Well Performance- Deliverability

2.3 Tubing Performance of a Well

Production rates at various bottomhole pressures are used to create the tubing performance curve which reflects the capability of the completion system to deliver production up the well bore to the separator.

Tubing performance or vertical lift performance (VLP) analysis of a well is important part of the well design procedure. It provides with data needed for selecting the well completion correctly corresponding to lifting methods and plays significant role in evaluation of well's performance. (Herriot Watt, 2011)

2.4 Gradient Curves

The pressure gradient in a pipe line or well bore is the summation of following components:

- Hydrostatic head
- Friction head

Thus, the total pressure gradient can be written as:

$$\frac{dp}{dl} = \left(\frac{dp}{dl}\right)_{hs} + \left(\frac{dp}{dl}\right)_{fr} \quad [2.1]$$

The hydrostatic component is due to the density of the travelling fluid mixture at each point in the system and it is a complex function of the relative velocity of the phases present. The gravity head loss is proportional to the fluid density corrected for slip which in turn depends on the flow regime and fluid viscosity.

The friction component is controlled by fluid viscosity and geometric factors such as pipe diameter and roughness. As in the majority of the oil field application, the gravitational component normally accounts for around 90% of the overall head loss, the total pressure drop function is not that much particularly sensitive to the value of the friction loss coefficient.

2.5 Pressure Traverse Curves

Very often pressure calculations are presented in the form of the so-called pressure-traverse curves. Calculation is performed for a specific tubing diameter, fluid properties and production rate. These curves usually represent estimate of pressure as a function of production measured depth and they are generated for series of gas-liquid ratios, water cut values, well-head pressures e.g. they have a key role in sensitivity analysis for any of constituting parameters.

3. Artificial Lift Methods

3.1 Pump Systems

Rod Pumps the most commonly used artificial lift method. This pumping system consists of a downhole plunger which oscillates up and down by a rod connected to a rotor at the surface. The plunger movement displaces produced fluid into the tubing via a pump consisting of suitably arranged travelling and standing valves mounted within a pump barrel.

Hydraulic Pumps use a highly pressurized fluid to:

1. Drive a downhole turbine or positive displacement pump or
2. Flow through a venturi or jet, creating a low-pressure area which produces an increased drawdown and inflow from the reservoir

Electric Submersible Pumps (ESP) utilizes a downhole centrifugal pump driven by an electric motor which is supplied with electric power via a cable that is long-drawn from the surface penetrates the wellhead and is strapped to the outside of the tubing.

Progressing Cavity Pumps (PCP) employs a helical, metal rotor rotating inside an elastomeric, double helical stator. The rotating action is supplied by downhole electric motor or by rotating rods. (Mauricio G. Prado)

3.2 Gas Lift

The gas lift method involves the supply/injection of pressurized gas at some downhole point in the tubing to aerate or lessen the fluid column, in order to reduce the average density of the fluid. Increased gas/liquid ratio passing through the port to the surface leads to the reduction of the hydrostatic pressure gradient into the tubing, which is the most significant factor of the pressure drop in vertical multiphase flow. In this way the average flowing density is decreased and finally the pressure at the bottom of the well is decreased generating or improving the drawdown and consequently the flow from reservoir to the well.

When liquid flow in vertical wells is considered, the hydrostatic head is the major component of the pressure loss since the fluid has to flow against the head whereas frictional loss which is rate dependent becomes vital only at very high flow rates. The injected gas also improves the liquid flow rate by the energy of expansion, introduced to the system due to the natural behavior of gas while exposed to pressure drop, which has positive effect on fluid flow towards the surface. (Hernandez, 2016)

The lifting of fluid can be accomplished by either continuous or intermittent gas injection.

In continuous gas lift, the flowing bottom-hole pressure remains constant for a specific set of conditions and is regarded as a steady state flow operation. (Schlumberger, Gas Lift Design and Technology, 1999)

In intermittent gas lift, the reservoir fluid is produced intermittently by displacing liquid slugs with high pressure injection gas. At intermittent lift the flowing bottom-hole pressure will vary with the particular operation time of one cycle in production. Economics are mainly dictating the design of any lift installation. Intermittent lift is applicable to low productivity wells with low reservoir pressure. (Schlumberger, Gas Lift Design and Technology, 1999)

In this thesis the continuous gas lift method is utilized. In continuous flow gas lift the compressed gas is introduced from the annulus to the tubing inside at a fixed rate, through a gas lift valve at a fixed depth. The continuous gas lift method is usually applied in wells which have high bottom-hole pressure relatively to their depths or/and with high productivity index. In this way the bottom-hole pressure is reduced.

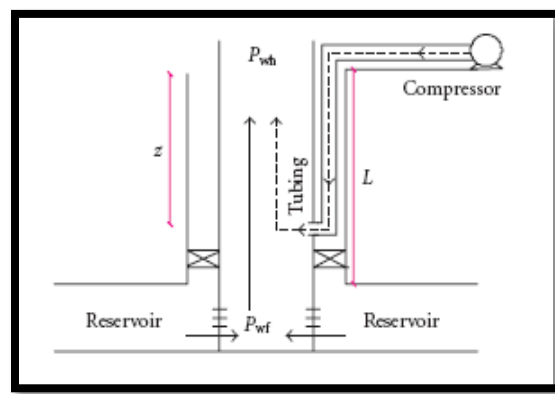


Figure 3.1 Simple Gas Lift Schematic (Deni et al, 2007)

3. Artificial Lift Methods

3.3 Gas lift equipment

The gas lift mechanism equipment can be divided into two main categories: the underground equipment and the surface one. As far as the surface equipment is concerned, a gas compressor is necessary in order to achieve the desired injection pressure. It is also necessary to have a multi-distribution (manifold) gas system consisting of a safety valve, a gas meter and a distribution column for each well. The underground equipment consists mainly of gas injection valves and the cases in which they are placed (mandrels). (Schlumberger, Gas Lift Design and Technology, 1999)

The gas injection valves are the tools installed along the tubing which allow the gas to enter the tubing and they are designed to open and close according to the pressure in the casing (IPO) or the Production column (PPO).

There are many types of gas injection valves in the market. Some are designed for use in continuous gas lift and some for intermittent. The force that closes the valve type of IPO, is generated by the nitrogen pressure contained within a chamber of the valve, which is called dome, while this force for valves type PPO it is supplied by a spring.

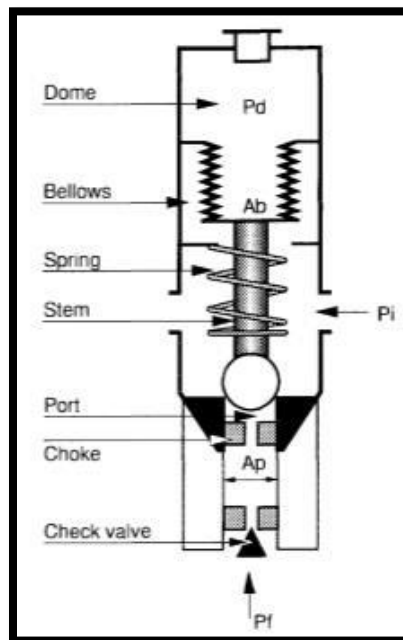


Figure 3.2 : Gas injection valve

3.3.1 Gas lift Advantages

The main advantages of the gas lift system are:

- A central gas lift system can be implemented when more than one well need it
- Gas lift is a method that can handle in the best way the sand and solid materials that enter the well while production
- Wells that are deviated can easily host a gas lift system
- It is a cost-effective method since the gas which is used is mainly the gas which solutes from the reservoir fluid

3.3.2 Gas Lift Disadvantages

The main disadvantages of the gas lift system are:

- In order to implement an efficient system good quality data are required
- The difficulty can be increased because of the friction
- The required gas is not always available

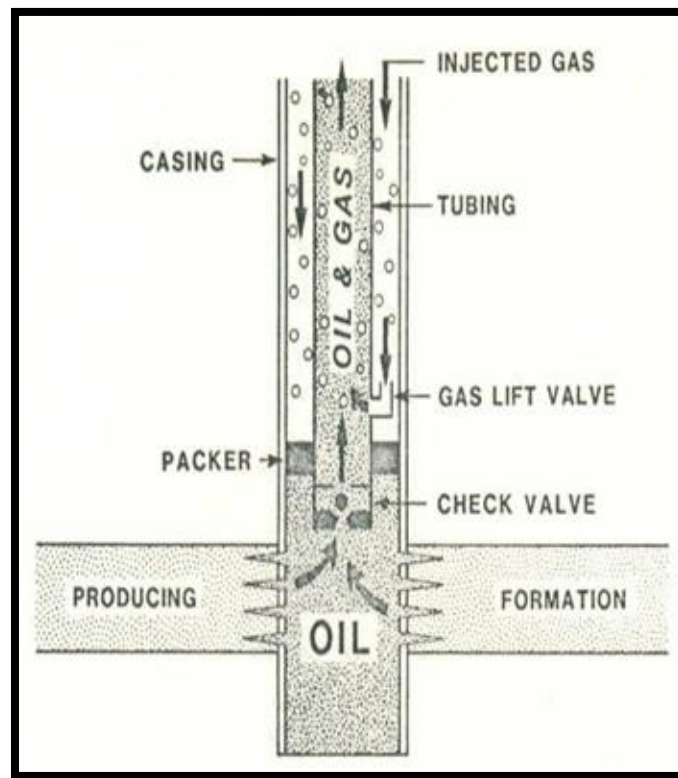


Figure 3.3 Artificial Gas lift system

4. Description of the Reservoir Model

The Reservoir model which is used in this Master thesis is the “Black Oil Demo” model, provided by the tNavigator reservoir simulation package of RFD, as part of the case studies for learning and training.

The Reservoir Model has been scheduled to operate nine producing wells and six water injection wells, which are controlled so as to deliver specific flowrates of liquid, as it can be seen in the Figure 4.1. During operating time, it can be easily observed that the pressure of the reservoir is being depleted at the early stages of production, until the injectors start water flooding. This results to the increase of water cut to most of the wells. Additionally, during the simulation run the producers start to operate at various times.

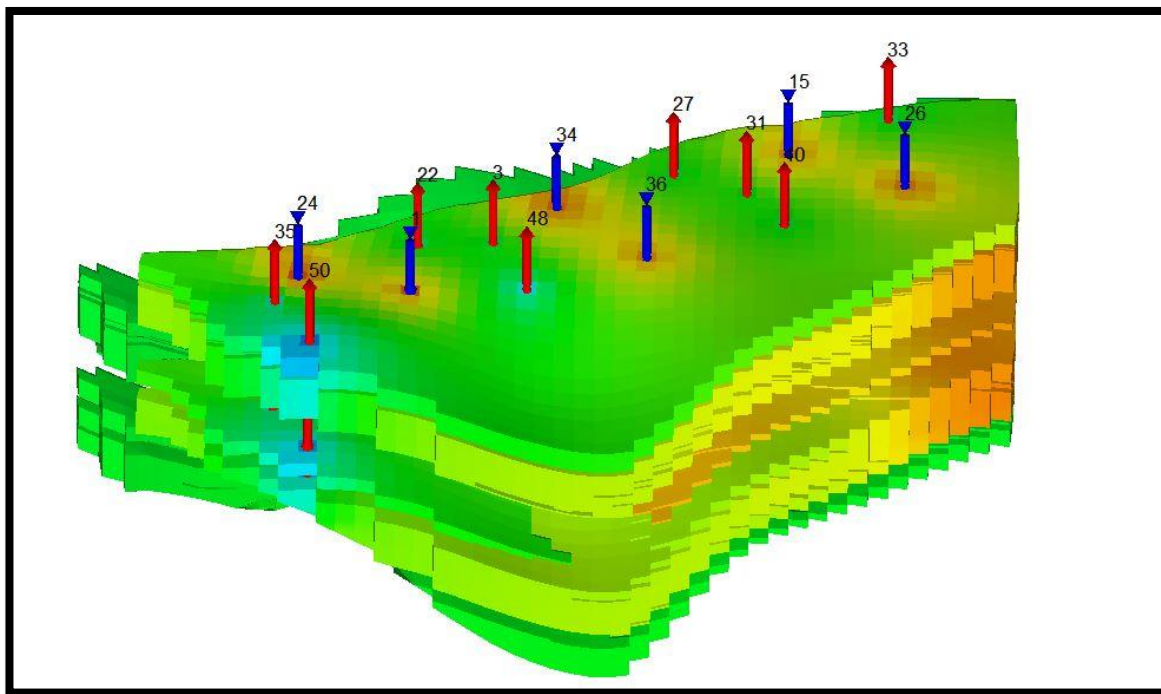


Figure 4.1 3D Map of the pressures of the Reservoir model (tNavigator, v4.1.3, 2015)

In Figure 4.1 we can visualize the reservoir shape and the location of the wells, whereas the water injector wells are in red color and the producers in blue.

In order to design the path of the wells it is needed to extract from the Reservoir model the distances that need to be covered by the wells' deviation survey. For this reason, the rig was selected to be placed close to the center of the reservoir footprint at the surface.

The distances of the well blocks from the rig that is positioned at block [28,19] can be seen below in Table 4.1.

PRODUCERS			
WELL	BLOCK	Horizontal distance(ft)	TOPS (ft)
3	22,20	1500.33	4676.02
22	18,20	2459.65	4676.12
27	31,12	1724.41	4663.39
31	35,14	2113.52	4670.60
33	42,6	4587.93	4651.12
35	11,27	4665.68	4684.25
40	37,17	2287.40	4679.27
48	24,24	1529.53	4693.04
50	13,31	4730.64	4694.82

Table 4:1 Horizontal distances of the wells from the rig

Finally, it is important the fact that the reservoir has two zones from which it is being produced and through which it is perforated. As the temperature value was missing from the model description, it was calculated at 150 °F by means of a typical geothermal gradient.

4.1 Fluid properties

The fluid properties utilized in the reservoir model are:

Regions	API	Sg	Specific Gravity of Water	GOR scf/stb
#1	38.41	0.94	1.012	218.968
#2	38	0.94	1.012	459.16

Table 4:2 Properties of the fluid

It can be seen, that the reservoir contains black oil since the GOR values are relatively low to medium, the API density is in the range of the black oils, and the specific gravity of the gas is relatively high. (Petrowiki, n.d.).

The initial saturation of water is defined as the amount of the water phase that exists in the rock pores by the time of the discovery. Although, it is commonly used as the irreducible water

4. Description of the Reservoir Model

saturation for which below that value the water cannot flow due to surface tension forces, in the model utilized S_{wi} is 23%. Subsequently, since the reservoir is undersaturated there is no gas phase and the existing phases are only water and oil, while the initial oil saturation is $1 - S_{wi}$ thus being equal to 0.77. In the graph below, the relative permeability curves of oil (red color) and of water (blue color) versus saturation are shown.

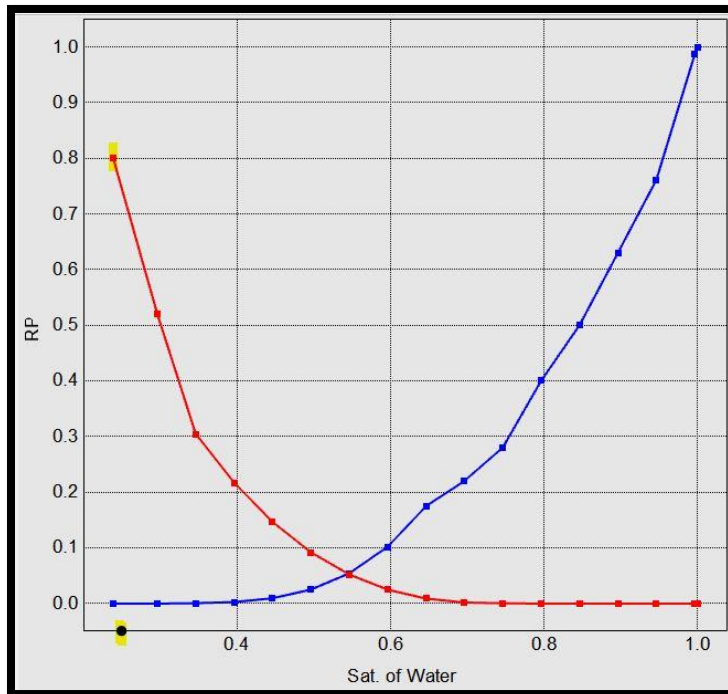


Figure 4.2 Relative Permeabilities Curves Water-Oil (tNavigator, v4.1.3, 2015)

4.2 Deviation Survey of the Wells

The wells are built in a build, hold and drop trajectory (called S-type) so as to penetrate the perforations vertically. With the information that has been obtained from the Reservoir model as far as the distances are concerned it is possible to design the well path.

For the deviation survey we assumed that the production casing is from the top to the bottom and no liners are used. As well as that the final vertical length of the starts from the top of the reservoir to the perforation's depth.

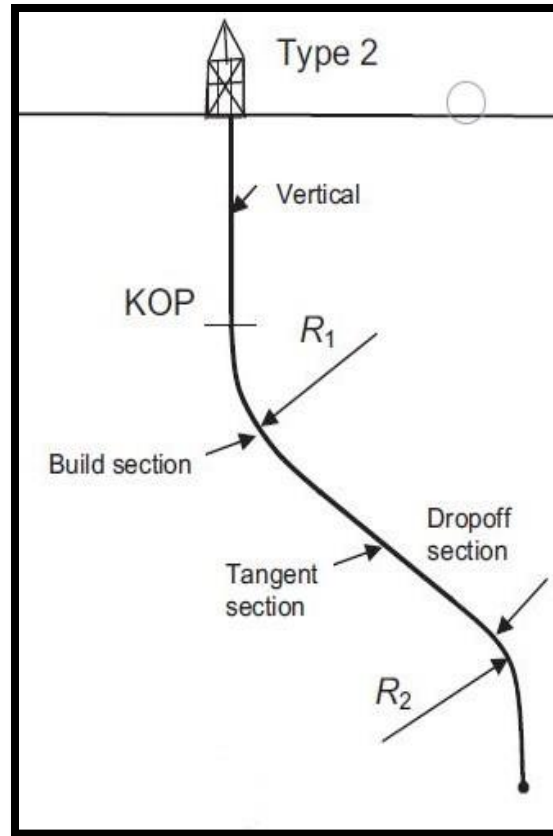


Figure 4.3 : Design of slant well type (Mitchell, 2011)

When the True Vertical Depth of each well's perforation is obtained from the software, we have to calculate the radius of curvature. For this reason, a rate of 3 deg/100ft is used.

$$r_1 = \frac{180}{\pi} \frac{1}{q} \quad (4.1)$$

In order to obtain the increments of various couples of TVD and MD, we used the following equations:

$$MD = KOP + \beta/q \quad (4.2)$$

$$TVD = KOP + R \cdot \sin(\beta) \quad (4.3)$$

KOP: kick off point, where the curvature starts,

4. Description of the Reservoir Model

R: radius of curvature,

β : slant angle,

When the slant angle was achieved, a tangential part was created until the point where a drop-off section equal to the buildup one would exist in order to reach the horizontal desired distance and revert back to a zero-inclination angle.

Subsequently, with this procedure we continued the calculations for all the producing wells and the following tables of True Vertical Depth and Measured Depth results were obtained.

W3		W22		W27		W31		W33	
TVD (ft)	MD (ft)								
0	0	0	0	0	0	0	0	0	0
800	800	800	800	800	800	800	800	800	800
847	847	886	886	856	856	868	868	952	951
895	895	973	973	912	912	935	935	1103	1102
942	942	1059	1058	969	969	1003	1003	1255	1251
989	989	1145	1144	1025	1024	1071	1070	1406	1396
1037	1036	1232	1228	1081	1080	1139	1137	1558	1538
1084	1083	1318	1312	1137	1136	1206	1203	1709	1676
1131	1130	1405	1395	1194	1191	1274	1269	1861	1808
1179	1176	1491	1476	1250	1246	1342	1335	2012	1933
1226	1223	1577	1556	1306	1300	1409	1399	2164	2051
1273	1269	1664	1635	1362	1354	1477	1463	2315	2162
1321	1315	1750	1712	1418	1408	1545	1526	2467	2264
1368	1360	1836	1787	1475	1461	1612	1589	2618	2357
1415	1405	1923	1860	1531	1514	1680	1650	2770	2440
1463	1450	2009	1931	1587	1565	1748	1710	2921	2512
1510	1494	2096	1999	1643	1617	1816	1769	3073	2574
1557	1538	2182	2065	1700	1667	1883	1827	3225	2625
1605	1582	2268	2129	1756	1717	1951	1883	3376	2664
1652	1624	2355	2189	1812	1766	2019	1938	3528	2691
1699	1667	2441	2247	1868	1814	2086	1992	3679	2707
4103	3809	3945	3229	4034	3649	3989	3479	4790	2777
4150	3852	4031	3287	4090	3698	4056	3532	4942	2793
4198	3894	4117	3348	4146	3747	4124	3587	5093	2820
4245	3938	4204	3411	4202	3796	4192	3644	5245	2860
4293	3982	4290	3477	4259	3847	4259	3702	5396	2910
4340	4026	4376	3546	4315	3898	4327	3761	5548	2972

4. Description of the Reservoir Model

4387	4071	4463	3616	4371	3950	4395	3821	5699	3045
4435	4116	4549	3689	4427	4002	4463	3882	5851	3128
4482	4161	4635	3764	4484	4055	4530	3944	6002	3220
4529	4207	4722	3841	4540	4109	4598	4007	6154	3322
4577	4253	4808	3920	4596	4163	4666	4071	6305	3433
4624	4300	4895	4000	4652	4218	4733	4136	6457	3551
4671	4346	4981	4081	4708	4272	4801	4201	6609	3677
4719	4393	5067	4164	4765	4328	4869	4267	6760	3809
4766	4440	5154	4248	4821	4383	4936	4334	6912	3946
4813	4487	5240	4332	4877	4439	5004	4401	7063	4088
4861	4534	5326	4418	4933	4495	5072	4468	7215	4234
4908	4581	5413	4504	4990	4551	5140	4535	7366	4382
4955	4629	5499	4590	5046	4607	5207	4603	7518	4533
5003	4676	5586	4676	5102	4663	5275	4671	7669	4684

Table 4:3 MD and TVD of the wells

W35		W40		W48		W50	
TVD (ft)	MD (ft)						
0	0	0	0	0	0	0	0
800	800	800	800	800	800	800	800
952	951	879	879	848	848	951	951
1103	1102	957	957	896	896	1102	1101
1255	1251	1036	1035	944	944	1252	1248
1406	1396	1114	1113	992	991	1403	1394
1558	1538	1193	1190	1039	1039	1554	1535
1709	1676	1272	1267	1087	1086	1705	1672
1861	1808	1350	1343	1135	1134	1856	1803
2012	1933	1429	1418	1183	1181	2007	1928
2164	2051	1507	1492	1231	1228	2157	2047
2315	2162	1586	1564	1279	1274	2308	2157
2467	2264	1665	1636	1327	1320	2459	2259
2618	2357	1743	1706	1375	1366	2610	2352
2770	2440	1822	1774	1423	1412	2761	2435
2921	2512	1900	1841	1471	1457	2912	2508
3073	2574	1979	1906	1518	1502	3062	2570
3225	2625	2057	1969	1566	1546	3213	2621
3376	2664	2136	2030	1614	1590	3364	2661
3528	2691	2215	2089	1662	1634	3515	2690
3679	2707	2293	2146	1710	1676	3666	2706
4790	2777	3965	3333	4118	3817	4841	2789

4. Description of the Reservoir Model

4942	2793	4044	3390	4166	3859	4992	2805
5093	2820	4123	3449	4214	3903	5143	2834
5245	2860	4201	3510	4262	3947	5293	2873
5396	2910	4280	3573	4310	3991	5444	2925
5548	2972	4358	3638	4358	4036	5595	2987
5699	3045	4437	3705	4406	4081	5746	3060
5851	3128	4515	3774	4454	4127	5897	3143
6002	3220	4594	3844	4502	4173	6048	3236
6154	3322	4673	3915	4550	4219	6198	3338
6305	3433	4751	3988	4597	4265	6349	3448
6457	3551	4830	4061	4645	4312	6500	3566
6609	3677	4908	4136	4693	4359	6651	3692
6760	3809	4987	4212	4741	4407	6802	3823
6912	3946	5066	4289	4789	4454	6953	3960
7063	4088	5144	4366	4837	4502	7103	4101
7215	4234	5223	4444	4885	4549	7254	4246
7366	4382	5301	4522	4933	4597	7405	4394
7518	4533	5380	4601	4981	4645	7556	4544
7669	4684	5459	4679	5029	4693	7707	4695

Table 4:4 MD and TVD of the wells

After the calculations were completed, the obtained deviation surveys were imported into the PIPESIM software. In the figures below, we can visualize the trajectories of the wells.

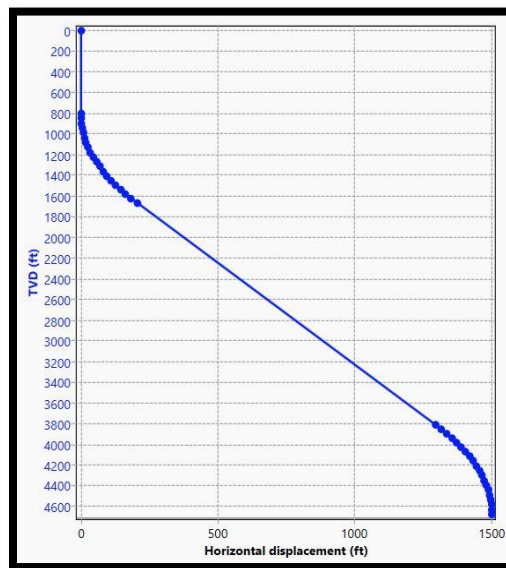


Figure 4.4 Deviation survey W3 (PIPESIM Steady-State Multiphase Flow Simulator)

4. Description of the Reservoir Model

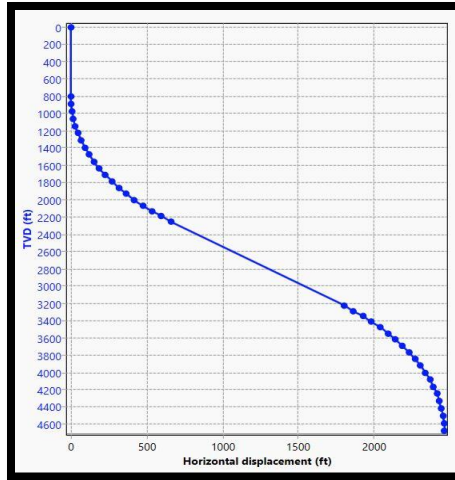


Figure 4.5 Deviation survey W22 (PIPESIM Steady-State Multiphase Flow Simulator)

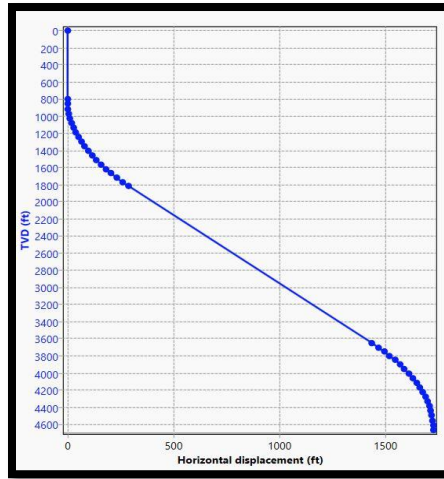


Figure 4.6 Deviation survey W27 (PIPESIM Steady-State Multiphase Flow Simulator)

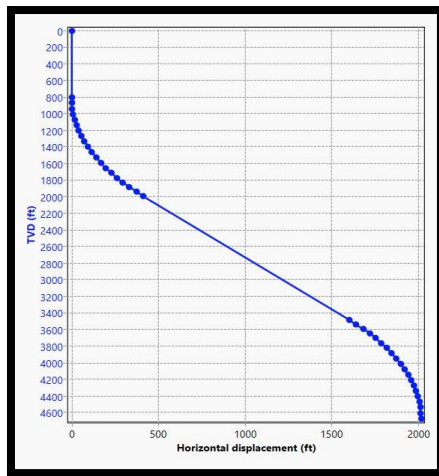


Figure 4.7 Deviation survey W31 (PIPESIM Steady-State Multiphase Flow Simulator)

4. Description of the Reservoir Model

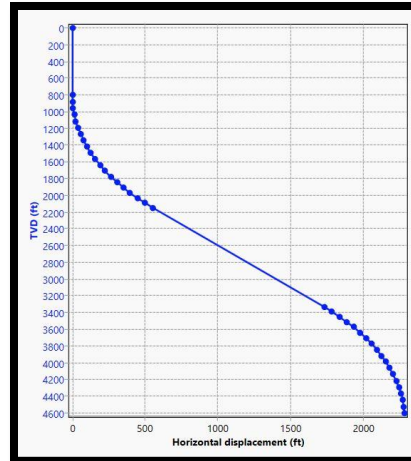


Figure 4.8 Deviation survey W33 (PIPESIM Steady-State Multiphase Flow Simulator)

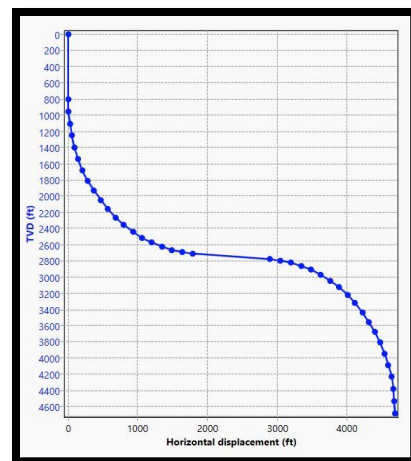


Figure 4.9 Deviation survey W35 (PIPESIM Steady-State Multiphase Flow Simulator)

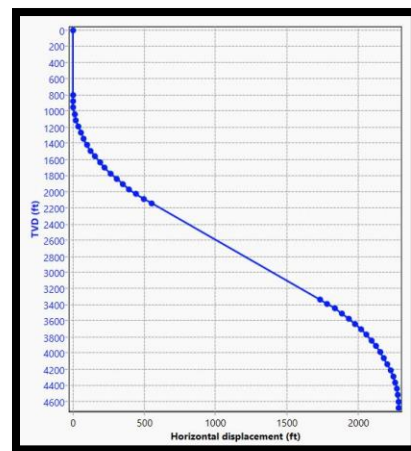


Figure 4.10 Deviation survey W40 (PIPESIM Steady-State Multiphase Flow Simulator)

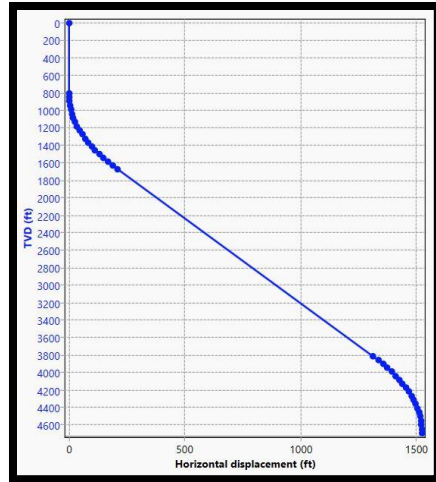


Figure 4.11 Deviation survey W48 (PIPESIM Steady-State Multiphase Flow Simulator)

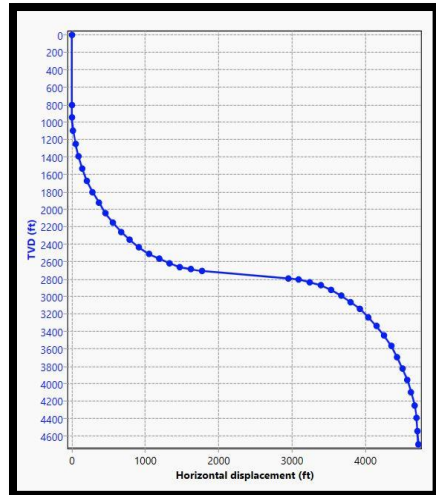


Figure 4.12 Deviation survey W50 (PIPESIM Steady-State Multiphase Flow Simulator)

4.3 Evaluation of wells' deliverability

In this paragraph we will take into account the results of the pressure traverse plots, that came out of the modeling in Pipesim, for the nine producing wells.

As mentioned before in Chapter 2, the pressure traverse curves are a common mean to estimate the pressure along the depth for certain conditions, and more specifically the pressure difference between the bottomhole and the wellhead, required to lift the liquids at surface. This way of estimating the pressures will be the guide for the current thesis in order to evaluate the wells' deliverability, as well as to decide for which wells and under which conditions, artificial gas lift

4. Description of the Reservoir Model

has to be designed. Therefore, a well to bring the production to the surface must exhibit a value at the end of the pressure traverse curve at least equal or lower to the bottomhole pressure under the conditions of investigation.

Practically, the PIPESIM software generates the pressure traverse plot for the conditions (e.g. flowrate, water cut) imposed by the reservoir model. The interpretation of the pressure traverse curves relies on the fact that the fluid must be able to overcome the difference of the pressure between the bottomhole and the wellhead. So, if the value at the end of the pressure traverse curve has bigger value than the reservoir model obtained bottomhole pressure, indicates that an artificial lift system must be installed. An example will be used to clarify the above statement, for the case that the well W3 has a reservoir model bottomhole pressure WBP=1296.5 psia and water cut WC=0.07%. In Figure 4.13 the pressure traverse plot is shown as it was generated from the PIPESIM software for the prevailing conditions.

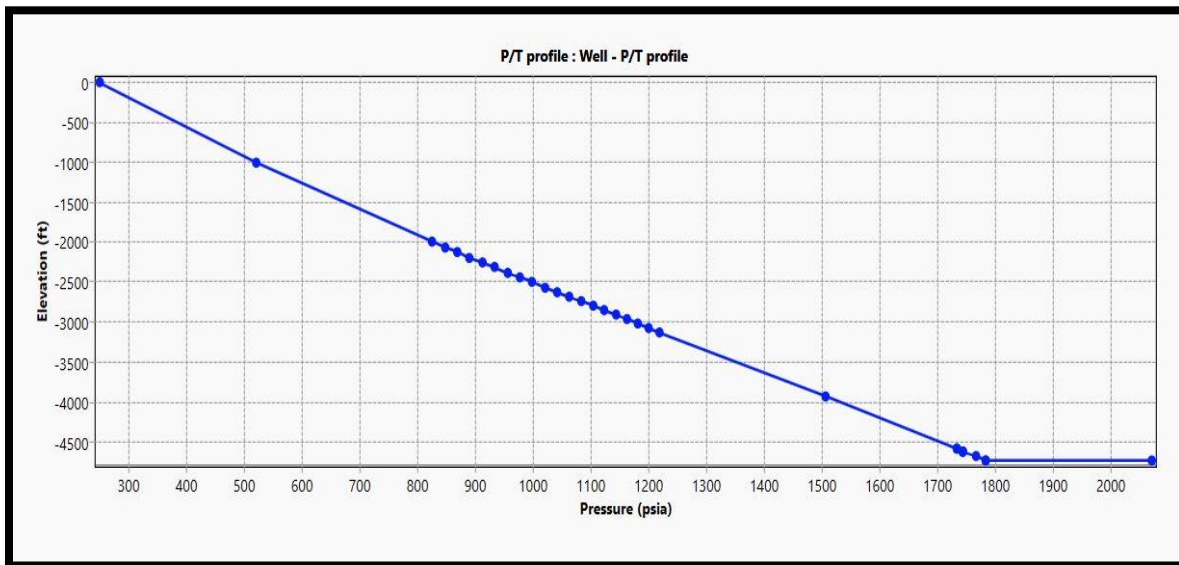


Figure 4.13 Pressure Traverse plot for well W3 (PIPESIM Steady-State Multiphase Flow Simulator, 2017)

The value at the end of the pressure traverse curve is of WBP=1789.3 psia which is well above the WBP of the reservoir model. In that case the pressure traverse curve implies that the well is not able to deliver the fluids from the reservoir to the wellhead and an artificial gas lift design must be implemented.

It must be taken into consideration that the well bottomhole pressures and the flowrates are fixed values, which were obtained from the reservoir simulation model.

The first condition that we investigated with the help of the pressure traverse plots is in the early stages of production for each well, that means when the water break-through occurs, with values much less than 1%. The results are shown in the Table 4.5.

WELL	WBP (psia)	PRESSURE TRAVERSE (psia)	WC%
W3	1296.5	1789.3	0.07%
W22	1344.0	1547.3	0.00%
W27	1219.0	1204.0	0.07%
W31	1488.4	1779.9	0.07%
W33	1118.7	1533.3	0.04%
W35	1104.3	1434.6	0.00%
W40	1361.2	1296.0	0.00%
W40	1511.5	1742.2	0.00%
W50	1436.0	1710.5	0.00%

Table 4:5 Results of Pressure Traverse curves for the wells

We can easily conclude that most of the wells are not able to deliver liquid to the surface and to respect the production rates determined by the reservoir modeling. Only two wells, W27 and W40 are able to bring the predicted oil and water rate to the surface by means of the predicted bottom hole pressure since they later exhibited higher pressure values than the computed endpoint pressure of the corresponding traverse curves.

4.3.1 Worst-case scenario

At this point, the worst-case scenario of the production schedule, will be identified and utilized in the study. If the gas lift system is designed so as to be able to cope with the worst-case scenario, that is the most difficult situation with respect to the available bottom hole pressure, then it can be guaranteed that it will be efficient for any other time instance during the production schedule of the reservoir. The worst-case scenario has been set to correspond to the situation of the highest

4. Description of the Reservoir Model

water cut level during the producing days for each well. The reason is that as the water fraction in the produced liquid grows the pressure loss due to gravity is becoming greater due to the higher density of the water compared to the oil, hence the increasing density of the produced liquid. Therefore, any other milder condition should be satisfied. According to this strategy, below is a list of the conditions of the worst-case scenarios which correspond to each well (Table 4.5).

Date	Pavg	WC%								
		W3	W22	W27	W31	W33	W35	W40	W48	W50
2/1/2015	2616.6	79.62%	47.38%	57.72%	80.67%	67.47%	80.44%	42.50%	43.25%	29.51%

Table 4:6 Worst case scenarios of the wells

WELL	WBP (psia)	Pressure at the end of Traverse curve (psia)	WC%
W3	1827.6	2174.8	79.62%
W22	1711.4	2069.3	47.38%
W27	2061.4	2050.5	57.72%
W31	2212.5	2234.8	80.67%
W33	1982.2	2032.7	67.47%
W35	1609.1	2194.8	80.44%
W40	2114.5	1439.4	42.50%
W48	1629.3	1870.4	43.25%
W50	1219.7	1768.9	29.51%

Table 4:7 Results of Pressure Traverse curves for the worst-case scenarios

In Table 4.7 between the comparison of the WBP and the value that the pressure traverse curves, it can be easily seen that only the wells W27 and W40 are able to produce according to the reservoir simulation schedule. So those two wells can deliver the fluid to the surface for the whole production time. For all other wells, it is shown that the bottom hole pressure is much less than the one that it should exhibit to ensure production. Hence, a gas lift design will be necessary and will be based for the worst-case scenarios since the rest of the wells are not able to produce from the early stages until the end of the exploitation of the field.

5. Gas Lift Design

The artificial gas lift procedure aims, either initiating the production in the tubing or enhancing the production that does not respect the economical limits of the reservoir simulation. Actually, gas lift design ensures that the bottomhole pressures that will allow the fluids to flow to the surface.

In this project, in order to design the gas lift system, we estimated the injection pressure values and the amount of the injection gas that was required.

5.1 Tubing Size Optimization

It was decided to run a sensitivity analysis to decide the best tubing size that will fit the production predictions.

When the inner diameter of the tubing increases, what it is achieved is better flowrate at a certain point. When the gas enters the tubing, it results to the decrease of the density of the fluid column. Hence, by increasing the inner diameter of the tubing more gas is expected to exist at the same depth with the liquid in the tubing, therefore the hydrostatic pressure decreases and the fluid column becomes lighter.

Additionally, when the gas that is injected occupies bigger area than the liquid itself then slip phenomenon start taking place in the tubing. Namely, to the fact that the gas flows faster than the liquids, the phenomenon that observed in this case will be the gas to be produced alone in the surface and the liquid to hold up, unable to move any more.

Been based on this principle we tried to find out the adequate tubing size for each well in order to deliver the desired amount of liquid to the surface as it was scheduled from the dynamic reservoir model.

5. Gas Lift Design

WELLS	Q _L sbbl/day
W3	1303.01
W22	738.56
W31	1776.52
W33	1779.71
W35	703.62
W48	958.85
W50	898.25

Table 5:1 Liquid flowrates prediction

5.1.1 Analysis for the tubing selection

As it was mentioned before, we ran an analysis to find the tubing size that will fit our production schedule. The general idea is the more the tubing inner diameter increase the better is the production flowrate. For this Master Thesis, with respect to that we made the tubing selection according to the target flowrate that must be achieved.

In this paragraph the optimum tubing size methodology will be examined that has been implemented. The procedure exhibited will be based in the worst-case scenario of the well W3 under the conditions of reservoir pressure $P_{avg} = 2616.6$ psia and water cut equal to $WC = 79.62\%$.

Hence, after we introduced the data regarding the properties of the fluids and the well deviation survey, we generated pressure traverse plot, to determine if the well can produce for the specific case. Below, in the Figure 5.1, it is shown the pressure traverse plot for the well W3, which will be the exhibition well to show the tubing selection procedure.

The well W3, under the worst-case scenario conditions is considered to have well bottom pressure, $WBP = 1827.6$ psia. In the plot which was obtained from the PIPESIM software, the pressure traverse gives pressure value equal to 2174.8 psia. So, according to the principle the well is not able to deliver fluids in the surface.

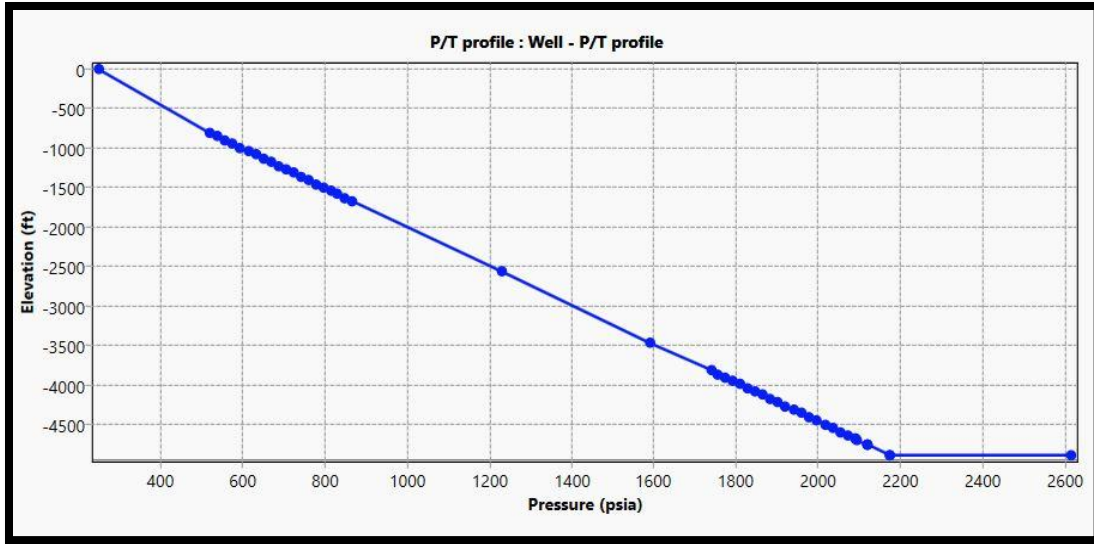


Figure 5.1 Pressure Traverse plot for the well W3 (PIPESIM Steady-State Multiphase Flow Simulator)

5.1.2 Input Data for the Gas Lift

The following tables consist the necessary input data that PIPESIM requires to process the gas lift design. These data are the output of the reservoir simulation and the designed deviation survey.

WELL DATA				
	MD (ft)	ID (in)	THICKNESS (in)	ROUGHNESS (in)
Casing	5447.6	7.511	0.557	0.001
Tubing	5000	2.441	0.375	0.001
PACKER	4800			

Table 5:2 Well Data for W3

FLUID MODEL	
WC %	79.62
GOR #1 (scf/stb)	218.98
GOR #2 (scf/stb)	459.16
S_g	0.94
Water gravity	1.012
API #1	38.41
API #2	38

Table 5:3 : Fluid properties for W3

RESERVOIR DATA

5. Gas Lift Design

P_{res} (psia)	2616.6
PI (stb/d.psi)	0.43
T (°F)	150

Table 5:4 Reservoir Data for W3

GAS LIFT DESIGN DATA	
Outlet Pressure (psia)	250
Q_{INJ} (mmscf/d)	1.035
S_g	0.64

Table 5:5 Gas Lift Design Data for W3

The Table 5.5 shows the data that are required in order to design the artificial gas lift in the PIPESIM software. The outlet pressure of the well is considered to be the pressure that exists at the wellhead, in the current case we assumed a typical value of 250 psia as wellhead pressure for the well W3 and the rest.

The injection flowrate is based on two criteria. Firstly, we use the needed amount of gas which is produced from the field, assuming that the cost of buying gas is not affordable. Secondly, we have to ensure that the amount of gas is available during the whole production period. So, the amount of the injected gas comes from the lowest gas production of the whole field and it is equal to 1.108 mmscf/day, at the last day of production (Figure 5.2). The injected amount of gas of each well is equal to the production of the last day subtracted the gas production of the under design well.

$$Q_{INJ,i} = Q_{TOT} - Q_i, \quad i = \text{each well}$$

$Q_{INJ,i}$, the gas injection flowrate for each well

Q_i , the gas produced from each well under the prevailing conditions

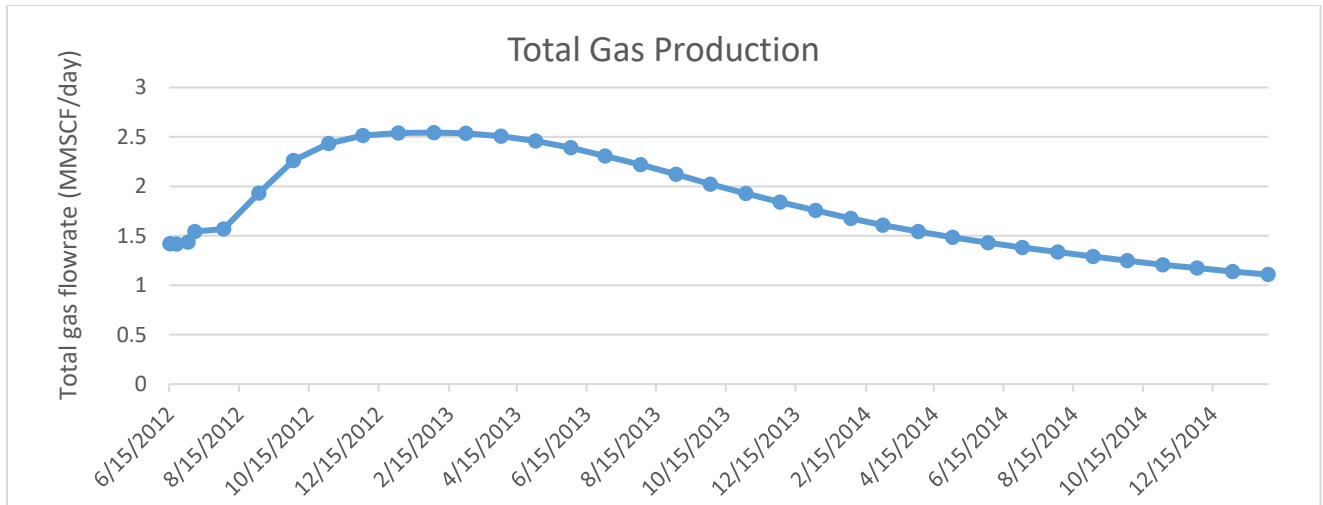


Figure 5.2 Total Gas production of the Field

5.1.3 Tubing Selection Methodology

The method used in order to find out which of the tubing inner diameter suits better the case of the well W3, follows a trial and error approach. In this approach we keep constant all the input data that were shown previously, such as deviation survey, reservoir data, well data, gas lift design data and fluid properties, but we keep changing the tubing inner diameter and the injection pressure, so as to achieve the target flowrate of 1303 sbbl/day.

The injection pressure plays significant role when the gas lift is designed, since it determines the deepest injection point. It is important to reach the deepest injection point in order to obtain less liquid hold up.

The procedure begins with constant diameter and variable injection pressure to reach the target flowrate. The same procedure was followed for the rest of the tubing inner diameters, in order to choose the suitable one which can deliver the requested amount of liquid. The appropriate tubing inner diameter of well W3 will be searched among 2.441, 2.75, 3.5, 4- and 5-inches.

The results of the above procedure can be shown in the next tables.

5. Gas Lift Design

ID=2.441 in						
P_{INJ} (psia)	500	700	800	900	1000	1050
Q_L (stb/d)	543.3	896.3	1056.1	1147.9	1233.4	1277.3
Q_{INJ} (mmscf/d)	1.035	1.035	1.035	1.035	1.035	1.035
P_{INJ} (psia)	1053	1054	1100	1200	1300	2000
Q_L (stb/d)	1278.6	1316.5	1316.6	1315.5	1315.7	1315.9
Q_{INJ} (mmscf/d)	1.035	1.035	1.035	1.035	1.035	1.035

Table 5:6 Gas lift of W3, tubing ID= 2.441in

ID=2.75 in						
P_{INJ} (psia)	500	700	800	900	905	907
Q_L (stb/d)	546.83	936.74	1197.21	1295.32	1299.97	1302.74
Q_{INJ} (mmscf/d)	1.035	1.035	1.035	1.035	1.035	1.035
P_{INJ} (psia)	909	910	1000	1100	1200	2000
Q_L (stb/d)	1303.28	1305.21	1381.11	1382.32	1382.31	1382.53
Q_{INJ} (mmscf/d)	1.035	1.035	1.035	1.035	1.035	1.035

Table 5:7 Gas lift of W3, tubing ID= 2.75in

ID=3.5 in					
P_{INJ} (psia)	500	700	750	790	791
Q_L (stb/d)	522.31	1167.98	1237.65	1291.87	1293.63
Q_{INJ} (mmscf/d)	1.035	1.035	1.035	1.035	1.035
P_{INJ} (psia)	792	800	900	1200	2000
Q_L (stb/d)	1362.31	1373.75	1488.52	1488.01	1488.12
Q_{INJ} (mmscf/d)	1.035	1.035	1.035	1.035	1.035

Table 5:8 Gas lift of W3, tubing ID= 3.5in

ID=4 in					
P_{INJ} (psia)	500	700	745	754	758
Q_L (stb/d)	520.35	1264.64	1277.61	1295.3	1300.14
Q_{INJ} (mmscf/d)	1.035	1.035	1.035	1.035	1.035
P_{INJ} (psia)	759	760	800	1300	2000
Q_L (stb/d)	1300.94	1367.06	1504.12	1529.64	1529.35
Q_{INJ} (mmscf/d)	1.035	1.035	1.035	1.035	1.035

Table 5:9 Gas lift of W3, tubing ID= 4in

ID=5 in					
P_{INJ} (psia)	500	700	710	711	713
Q_L (stb/d)	521.45	1284.33	1295.27	1356.15	1377.11
Q_{INJ} (mmscf/d)	1.035	1.035	1.035	1.035	1.035
P_{INJ} (psia)	725	750	800	1300	2000
Q_L (stb/d)	1398.86	1441.51	1572.55	1571.48	1571.76
Q_{INJ} (mmscf/d)	1.035	1.035	1.035	1.035	1.035

Table 5:10 Gas lift of W3, tubing ID= 5in

As the above tables clearly show the tubing inner diameter of 2.441, 3.5 and 5 inches cannot reach a value as close as the reservoir simulation indicated flowrate. The tubing size of 2.75 inches delivers 1303.28 sbbl/day whereas the 4 inches delivers 1300.93 sbbl/day. Since the requested flowrate is a fixed value equal to 1303.01 the corresponding tubing diameter is 2.75 inches, with injection pressure of 909 psia and injection rate of 1.035 mmscf/day. Likewise, this method was implemented for all the wells of the field.

5.1.4 Conclusion

In Figure 5.4 it can be seen the plot of the injection pressures versus the produced liquid flowrate for all the tubing inner diameter cases concerning the well W3.

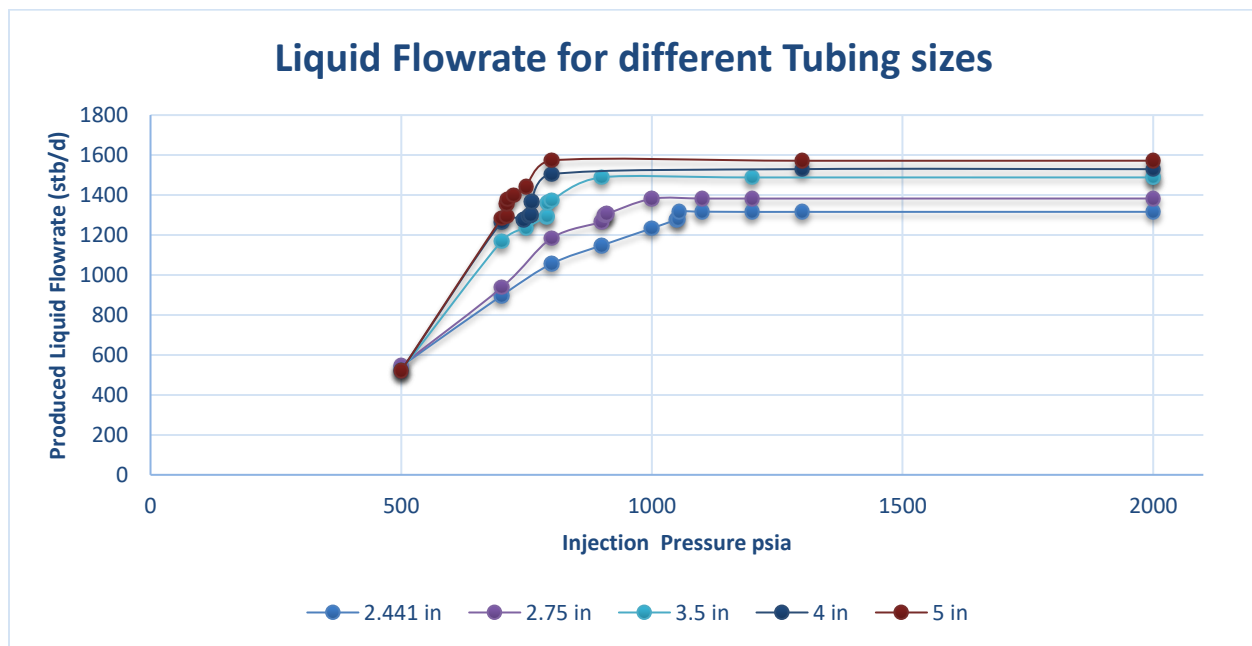


Figure 5.3 Liquid flowrate for different tubing sizes (well W3)

5. Gas Lift Design

It can be concluded that the produced liquid flowrate increases with respect to the increase of the tubing inner diameter and the injection pressure. Namely, the increase of the tubing size increases the liquid flowrate because the pressure loss is being reduced due to the frictional component decrease.

Furthermore, the injection pressure increase has significant effect on the liquid production up to a point that does not change further (plateau effect). That happens because the bigger the injection pressure is, the deeper the injection point the gas can reach. As a result, the fluid column becomes lighter, since the density of the gas is lower than the liquid.

5.1.5 Evaluation of the Gas lift design

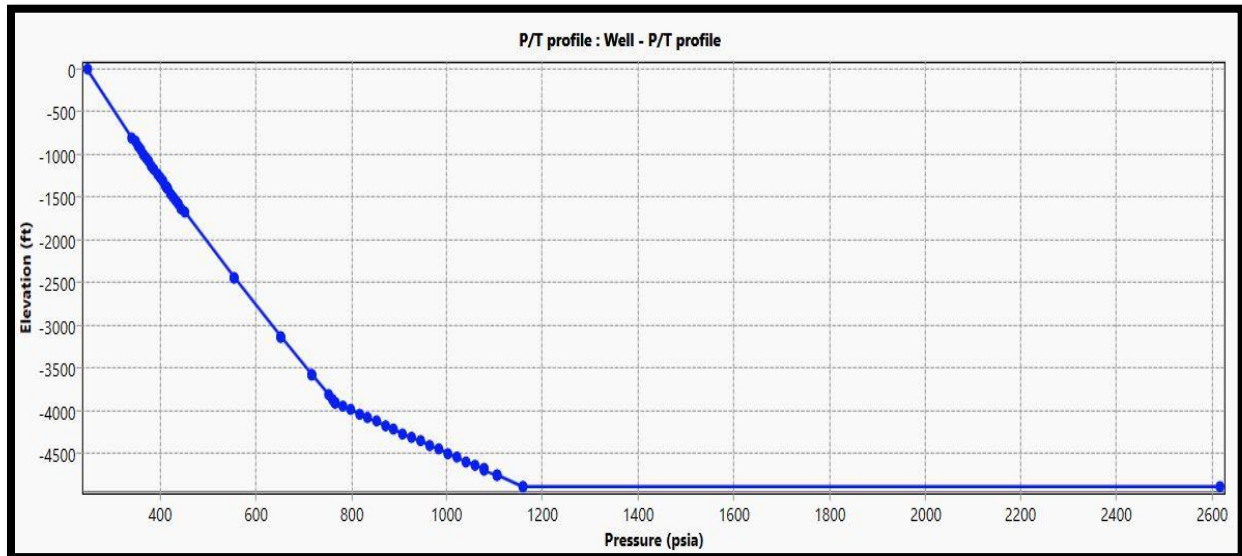


Figure 5.4 Pressure Traverse Plot after the Gas Lift installation (PIPESIM Steady-State Multiphase Flow Simulator)

In Figure 5.3 can be seen the pressure traverse curve as it was generated after the installation of the optimum gas lift design with respect to the appropriate tubing size. This plot evaluates the well performance of the installed gas lift system and it can be judged as successful, since it has achieved the desired flowrate as well as the pressure at the end of the traverse curve is 1159.1 psia, less than the WBP pressure (=1827.6 psia).

5.1.6 Gas lift design equipment for well W3

Figures 5.4-5.5 shows the artificial gas lift data and the visualization of the well after the implementation of the system respectively.

Gas lift	Active	MD ft	Manufacturer	Series	Valve type	Port size in	Ptro psia	St psia	Discharge coe...	DP to fully open psia
1	<input checked="" type="checkbox"/>	1393.235	SLB (Camco)	R20	IPO	0.25	957.9653		0.76	529
2	<input checked="" type="checkbox"/>	2568.542	SLB (Camco)	R20	IPO	0.25	966.4521		0.76	529
3	<input checked="" type="checkbox"/>	3341.238	SLB (Camco)	R20	IPO	0.25	966.9497		0.76	529
4	<input checked="" type="checkbox"/>	3842.439	SLB (Camco)	R20	IPO	0.25	961.9968		0.76	529
5	<input checked="" type="checkbox"/>	4203.062	SLB (Camco)	R20	IPO	0.3125	992.8749		0.76	443.2

Figure 5.5 Artificial Gas Lift equipment (PIPESIM Steady-State Multiphase Flow Simulator, 2017)

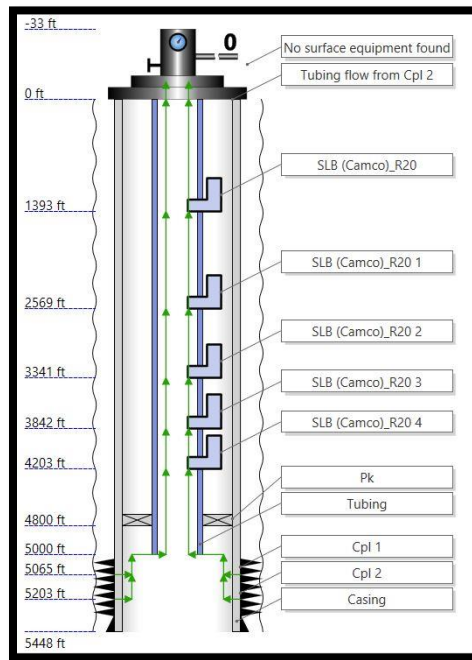


Figure 5.6 Gas Lift visualization for the Well W3 (PIPESIM Steady-State Multiphase Flow Simulator, 2017)

5. Gas Lift Design

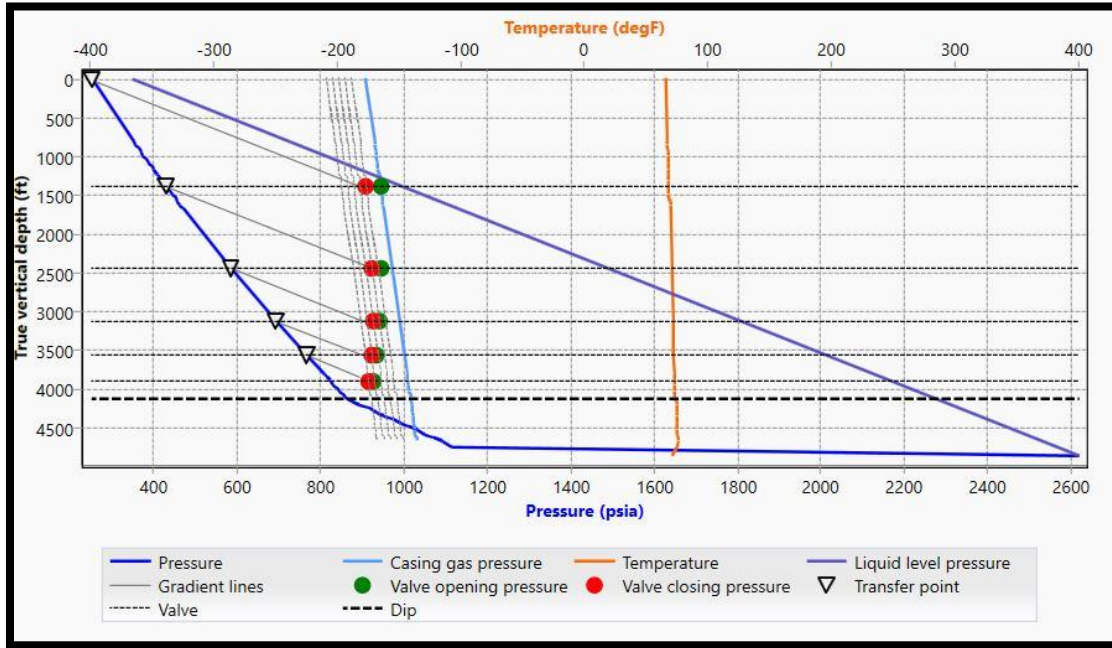


Figure 5.7 Pressure vs Depth of the Gas Lift installation (PIPESIM Steady-State Multiphase Flow Simulator, 2017)

Figure 5.6 indicates that five valves are installed along the tubing. The valves enable the access of the gas to enter from the annulus to the tubing. PIPESIM has the option to suggest the optimum way of valves' installation, under the conditions given by the user. Moreover, PIPESIM suggests the number of valves, the deepest injection point and the valves' spacing which suit best for its configuration.

6. Results of the Gas lift design

According to Chapter 5, the same procedure was followed for all the wells in order to choose the suitable tubing size. In addition, through this tubing selection methodology we are able to choose the appropriate injection pressures that will fit and complete the gas lift design. Below the results for all the wells are presented after the gas lift installation.

W3		
Reservoir Data	P_{avg} (psia)	2616.6
	PI sbbl/day/psia	0.433
	WC%	79.62
	WBP (psia)	1827.65
	Q_L sbbl/day	1303.01
Gas Lift Output	ID (in)	2.75
	Q_L sbbl/day	1303.28
	P_{inj}(psia)	909

Table 6:1 Gas lift results for well W3

W22		
Reservoir Data	P_{avg} (psia)	2616.6
	PI sbbl/day/psia	0.392
	WC%	47.38
	WBP (psia)	1711.4
	Q_L sbbl/day	738.56
Gas Lift Output	ID (in)	2.441
	Q_L sbbl/day	738.52
	P_{inj}(psia)	544

Table 6:2 Gas lift results for well W22

6.Results of the Gas lift design

W31		
Reservoir Data	P_{avg} (psia)	2616.6
	PI sbbl/day/psia	0.595
	WC%	80.67
	WBP (psia)	2212.5
	Q_L sbbl/day	1776.52
Gas Lift Output	ID (in)	3
	Q_L sbbl/day	1776.62
	P_{inj}(psia)	961.5

Table 6:3 Gas lift results for well W31

W33		
Reservoir Data	P_{avg} (psia)	2616.6
	PI sbbl/day/psia	0.837
	WC%	67.47
	WBP (psia)	1982.2
	Q_L sbbl/day	1779.71
Gas Lift Output	ID (in)	4
	Q_L sbbl/day	1779.56
	P_{inj}(psia)	830.5

Table 6:4 Gas lift results for well W33

W35		
Reservoir Data	P_{avg} (psia)	2616.6
	PI sbbl/day/psia	0.113
	WC%	80.44
	WBP (psia)	1609.08
	Q_L sbbl/day	703.62
Gas Lift Output	ID (in)	5.5
	Q_L sbbl/day	594.98
	P_{inj}(psia)	2000

Table 6:5 Gas lift results for well W35

W48		
Reservoir Data	P_{avg} (psia)	2616.6
	PI sbbl/day/psia	0.501
	WC%	43.25%
	WBP (psia)	1629.3
	Q_L sbbl/day	958.85
Gas Lift Output	ID (in)	3
	Q_L sbbl/day	958.82
	P_{inj}(psia)	594

Table 6:6 Gas lift results for well W48

6.Results of the Gas lift design

W50		
Reservoir Data	P_{avg} (psia)	2616.6
	PI sbbbl/day/psia	0.341
	WC%	25.51
	WBP (psia)	1219.7
	Q_L sbbbl/day	898.25
Gas Lift Output	ID (in)	3
	Q_L sbbbl/day	898.62
	P_{inj}(psia)	709

Table 6:7 Gas lift results for well W50

According to the above results it can be stated that the artificial gas lift design generated by the PIPESIM software was overall successful. Under these configurations, the gas lift installation at the wells is able to deliver almost the exact daily liquid flowrate, requested by the reservoir simulation, with the least possible deviations from the predictions. It can be recognized by the table 6.8 that the deviation between the predicted production and the production achieved after the gas lift, is of minor importance and less than 1%.

WELLS	Deviation of Q_L from the predicted
W3	0.021%
W22	0.070%
W31	0.006%
W33	0.008%
W35	15.44%
W48	0.004%
W50	0.041%

Table 6:8 Deviation between the predicted and calculated production

In contradiction with the performance of the most of the wells, it is more than obvious that the well W35 seems that is not be able to fulfill the requirements of the production prediction, even after lift help. The scheduled flowrate should reach 703.6 sbbl/day but after the gas lift system implementation the achieved maximum rate, was 594 sbbl/day.

The design of the well W35 was made to the hilt with tubing size of 5.5 inches inner diameter, as it is limited from the casing size of 7.511 inches inner diameter. Moreover, it reaches a high injection pressure of 2000 psia. It seems that the gas lift is not suitable way of artificial lift for this well and probably an ESP pump could be investigated for installation. Recall that the well W35 reaches the highest water cut of 80.44% and apparently the fluid column is heavy enough and incapable to fit the provision.

7. Conclusion

The scope of the present thesis was to evaluate the wells' productivity in order to estimate if the wells of the reservoir model were able to deliver the desired daily liquid flowrate to the surface.

The Pressure traverse investigation showed that most of the wells were not able to produce what was scheduled. So artificial gas lift system was implemented to provide the needed energy to the system to lift the liquid. The gas lift system was selected to be designed under the worst-case scenario for the wells. This scenario exhibits the highest water cut values since the wells are unable to produce from their early stages of life.

The gas lift system was planned after the optimum tubing size which was respective to the liquid flowrate values. After the tubing size investigation, we are able to conclude to general judgments since we witnessed the effect of the injection pressure and the tubing size at the same time.

Generally, as the injection pressure is growing, we are able to achieve higher flowrates due to the deeper injection point we reach at the well. As well as the bigger the tubing inner diameter, the more efficient -in terms of production- becomes the well. The slip phenomenon which was expected to appear with the increasing diameter of the tubing was not the case of this study since the quantity of the injected gas was low.

The results of the design can be determined as successful, considering the matching of the predicted flowrates. Only one well was unsuccessful to deliver the exact fluid amount to the surface for which we claimed that could be assisted with additional artificial lift like an ESP pump.

To conclude with, when the reservoir energy is not sufficient to supply the fluids to come to the surface, then artificial gas lift design can be implemented as a cost-effective method for the industry compared to others.

Bibliography

- 1) Deni et al, S. &. (2007). An Investigation on Gas Lift Performance Curve in an Oil-Producing Well. *International Journal of Mathematics and Mathematical Sciences*.
- 2) H. Dale Beggs. (2008). *Production Optimization Using Nodal Analysis*.
- 3) Hernandez, A. (2016). *Fundamentals of Gas Lift Engineering: Well Design and Troubleshooting*.
- 4) Herriot Watt. (2005). *Reservoir Engineering* . Edinburg.
- 5) Herriot Watt. (2011). *Production Technology I*.
- 6) Kermit E. Brown, James F. Lea. (1985). *Nodal Systems Analysis of Oil and Gas Wells*.
- 7) Mauricio G. Prado. (n.d.). *Artificial Lift Methods, Introduction*. The University of Tulsa.
- 8) Mitchell, F. R. (2011). *Fundamentals of Drilling engineering*. Society of Petroleum Engineers.
- 9) Petrowiki. (n.d.). Retrieved from https://petrowiki.org/Oil_fluid_characteristics
- 10) RFDynamics. (2015). *tNavigator, v4.1.3*.
- 11) Schlumberger. (1999). *Gas Lift Design and Technology*.
- 12) Schlumberger. (2017). *PIPESIM Steady-State Multiphase Flow Simulator*.
- 13) Schlumberger. (2017). *PIPESIM user Manual*.

8. APPENDIX

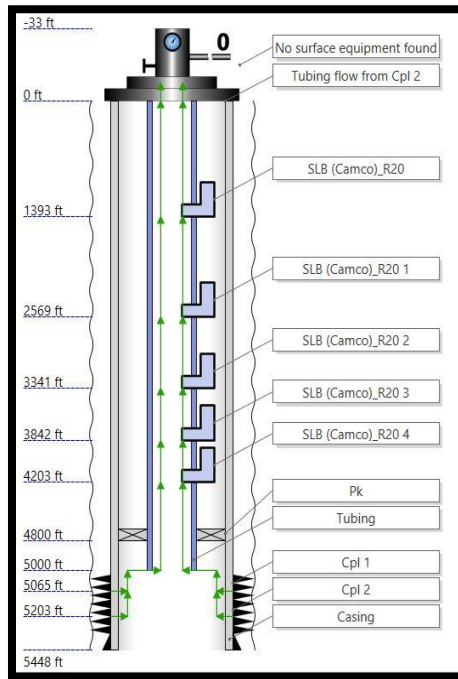


Figure 8.1 Artificial lift configuration for well W3

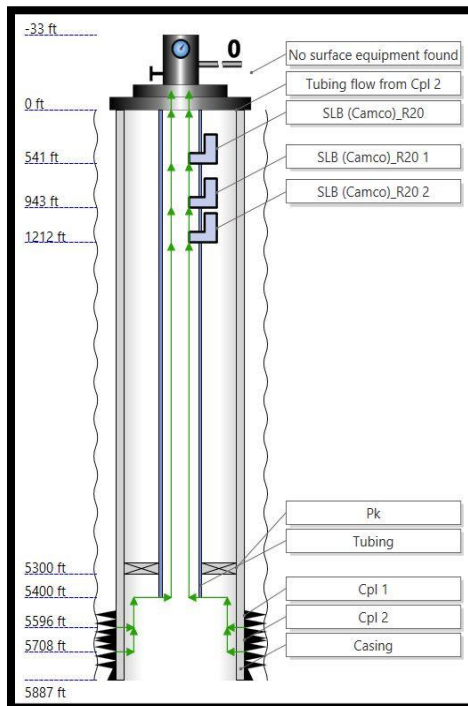


Figure 8.2 Artificial lift configuration for well W22

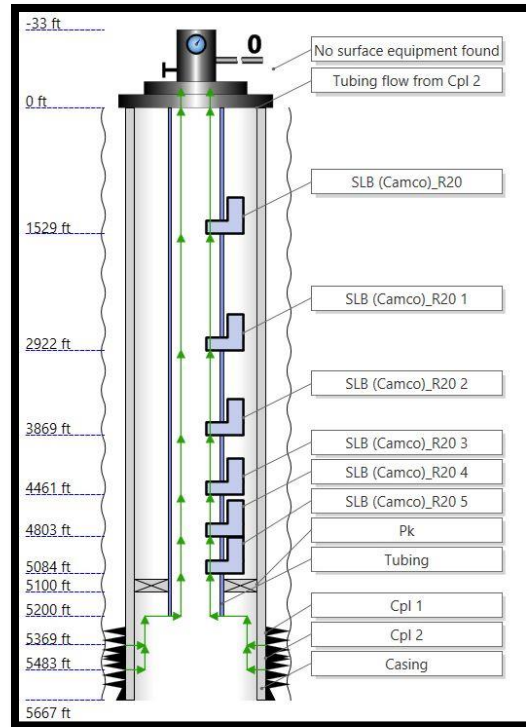


Figure 8.3 Artificial lift configuration for well W31

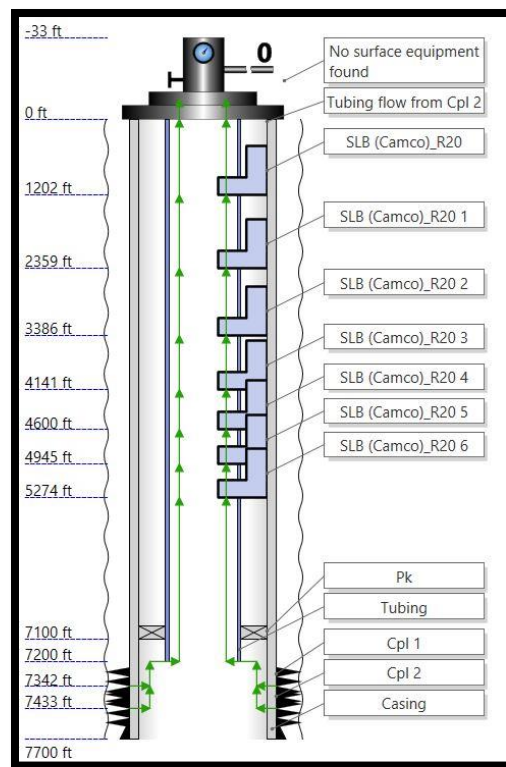


Figure 8.4 Artificial lift configuration for well W33

8.APPENDIX

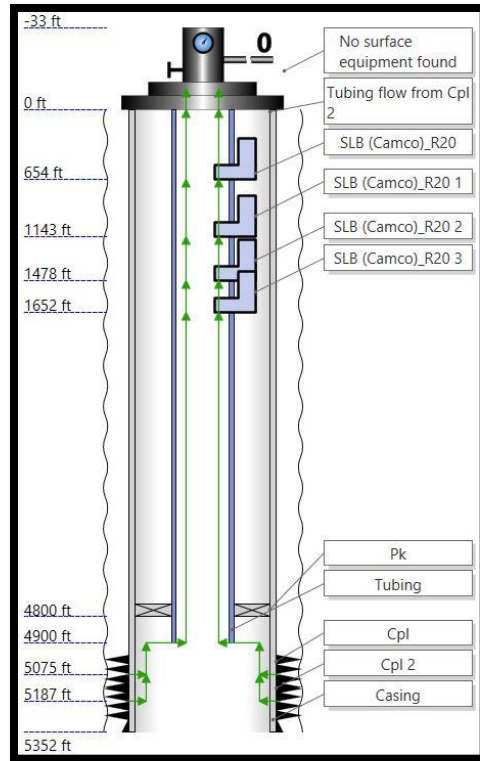


Figure 8.5 Artificial lift configuration for well W48

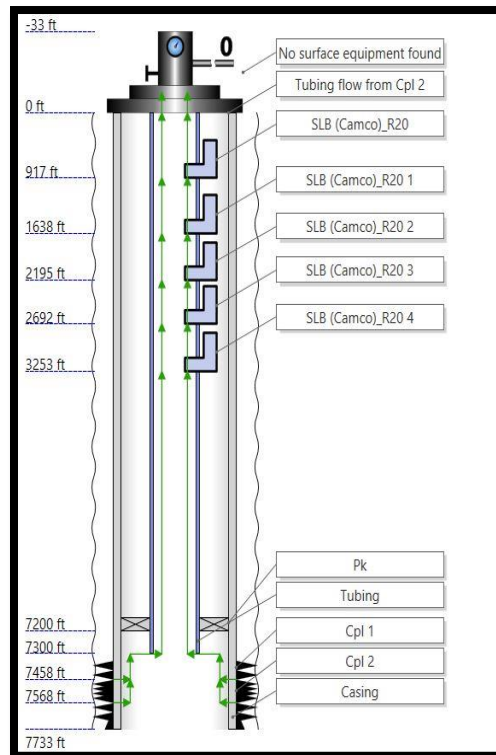


Figure 8.6 Artificial lift configuration for well W50

	Gas lift	Active	MD ft	Manufacturer	Series	Valve type	Port size in	Ptro psia	St psia	Discharge coe...	DP to fully open psia	
1	SLB (Camco)_...	<input checked="" type="checkbox"/>	540.8377	SLB (Camco)	R20	IPO	0.25	570.3163		0.76	529	...
2	SLB (Camco)_...	<input checked="" type="checkbox"/>	942.7349	SLB (Camco)	R20	IPO	0.25	559.1955		0.76	529	...
3	SLB (Camco)_...	<input checked="" type="checkbox"/>	1212.109	SLB (Camco)	R20	IPO	0.375	597.0301		0.76	382.6	...
+												

Figure 8.7 Artificial lift equipment W22

	Gas lift	Active	MD ft	Manufacturer	Series	Valve type	Port size in	Ptro psia	St psia	Discharge coe...	DP to fully open psia	
1	SLB (Camco)_...	<input checked="" type="checkbox"/>	1529.304	SLB (Camco)	R20	IPO	0.25	1036.371		0.76	529	...
2	SLB (Camco)_...	<input checked="" type="checkbox"/>	2922.483	SLB (Camco)	R20	IPO	0.25	1048.116		0.76	529	...
3	SLB (Camco)_...	<input checked="" type="checkbox"/>	3869.183	SLB (Camco)	R20	IPO	0.25	1050.662		0.76	529	...
4	SLB (Camco)_...	<input checked="" type="checkbox"/>	4461.132	SLB (Camco)	R20	IPO	0.25	1047.222		0.76	529	...
5	SLB (Camco)_...	<input checked="" type="checkbox"/>	4803.171	SLB (Camco)	R20	IPO	0.25	1039.497		0.76	529	...
6	SLB (Camco)_...	<input checked="" type="checkbox"/>	5084.251	SLB (Camco)	R20	IPO	0.3125	1072.446		0.76	443.2	...
+												

Figure 8.8 Artificial lift equipment W31

	Gas lift	Active	MD ft	Manufacturer	Series	Valve type	Port size in	Ptro psia	St psia	Discharge coe...	DP to fully open psia	
1	SLB (Camco)_...	<input checked="" type="checkbox"/>	1201.869	SLB (Camco)	R20	IPO	0.25	875.1407		0.76	529	...
2	SLB (Camco)_...	<input checked="" type="checkbox"/>	2358.652	SLB (Camco)	R20	IPO	0.25	880.2301		0.76	529	...
3	SLB (Camco)_...	<input checked="" type="checkbox"/>	3385.698	SLB (Camco)	R20	IPO	0.25	879.9735		0.76	529	...
4	SLB (Camco)_...	<input checked="" type="checkbox"/>	4140.616	SLB (Camco)	R20	IPO	0.25	875.9357		0.76	529	...
5	SLB (Camco)_...	<input checked="" type="checkbox"/>	4600.472	SLB (Camco)	R20	IPO	0.25	868.7222		0.76	529	...
6	SLB (Camco)_...	<input checked="" type="checkbox"/>	4945.305	SLB (Camco)	R20	IPO	0.25	860.2342		0.76	529	...
7	SLB (Camco)_...	<input checked="" type="checkbox"/>	5273.677	SLB (Camco)	R20	IPO	0.3125	886.3712		0.76	443.2	...
+												

Figure 8.9 Artificial lift equipment W33

	Gas lift	Active	MD ft	Manufacturer	Series	Valve type	Port size in	Ptro psia	St psia	Discharge coe...	DP to fully open psia	
1	SLB (Camco)_...	<input checked="" type="checkbox"/>	6398.424	SLB (Camco)	R20	IPO	0.25	2289.435		0.76	529	...
2	SLB (Camco)_...	<input checked="" type="checkbox"/>	7191.677	SLB (Camco)	R20	IPO	0.25	2292.208		0.76	529	...
+												

Figure 8.10 Artificial lift equipment W35

	Gas lift	Active	MD ft	Manufacturer	Series	Valve type	Port size in	Ptro psia	St psia	Discharge coe...	DP to fully open psia	
1	SLB (Camco)_...	<input checked="" type="checkbox"/>	653.7766	SLB (Camco)	R20	IPO	0.25	623.6489		0.76	529	...
2	SLB (Camco)_...	<input checked="" type="checkbox"/>	1142.975	SLB (Camco)	R20	IPO	0.25	614.2642		0.76	529	...
3	SLB (Camco)_...	<input checked="" type="checkbox"/>	1477.696	SLB (Camco)	R20	IPO	0.25	602.7532		0.76	529	...
4	SLB (Camco)_...	<input checked="" type="checkbox"/>	1652	SLB (Camco)	R20	IPO	0.375	643.9772		0.76	382.6	...
+												

Figure 8.11 Artificial lift equipment W48

8.APPENDIX

	Gas lift	Active	MD ft	Manufacturer	Series	Valve type	Port size in	Ptro psia	St psia	Discharge coe...	DP to fully open psia	
1	SLB (Camco)_...	<input checked="" type="checkbox"/>	916.8637	SLB (Camco)	R20	IPO	0.25	749.9427		0.76	529	...
2	SLB (Camco)_...	<input checked="" type="checkbox"/>	1638.142	SLB (Camco)	R20	IPO	0.25	745.6745		0.76	529	...
3	SLB (Camco)_...	<input checked="" type="checkbox"/>	2195.245	SLB (Camco)	R20	IPO	0.25	737.7045		0.76	529	...
4	SLB (Camco)_...	<input checked="" type="checkbox"/>	2691.871	SLB (Camco)	R20	IPO	0.25	727.4505		0.76	529	...
5	SLB (Camco)_...	<input checked="" type="checkbox"/>	3253.288	SLB (Camco)	R20	IPO	0.375	781.842		0.76	382.6	...

Figure 8.12 Artificial lift equipment W50

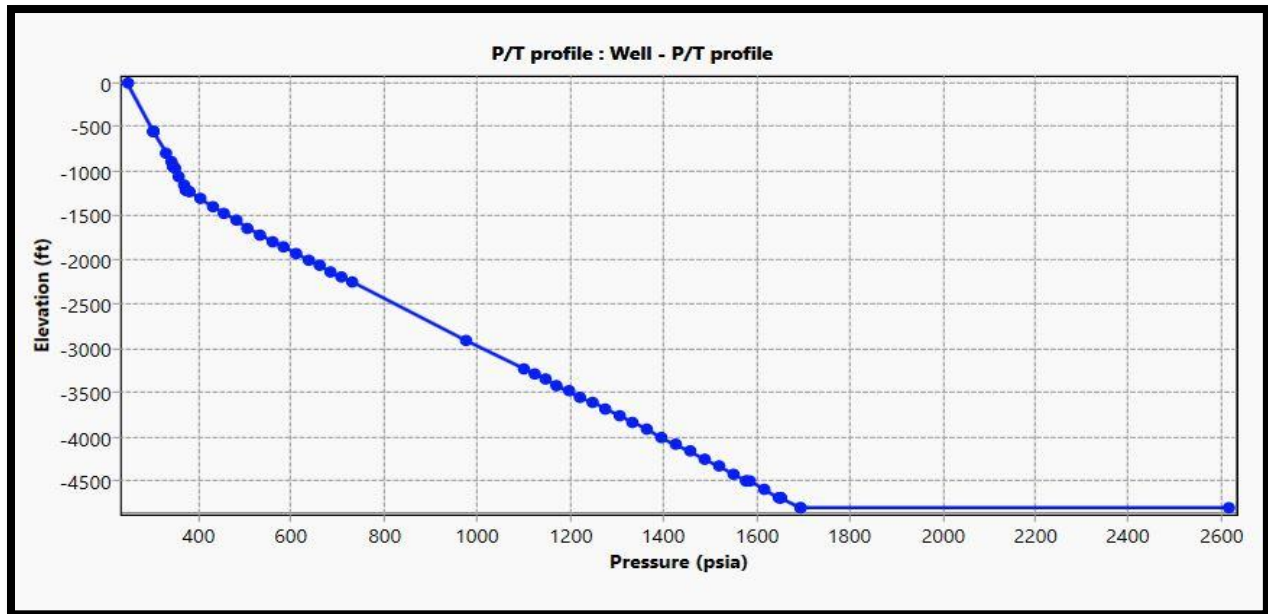


Figure 8.13 Pressure Traverse Curve after Gas Lift installation for well W22

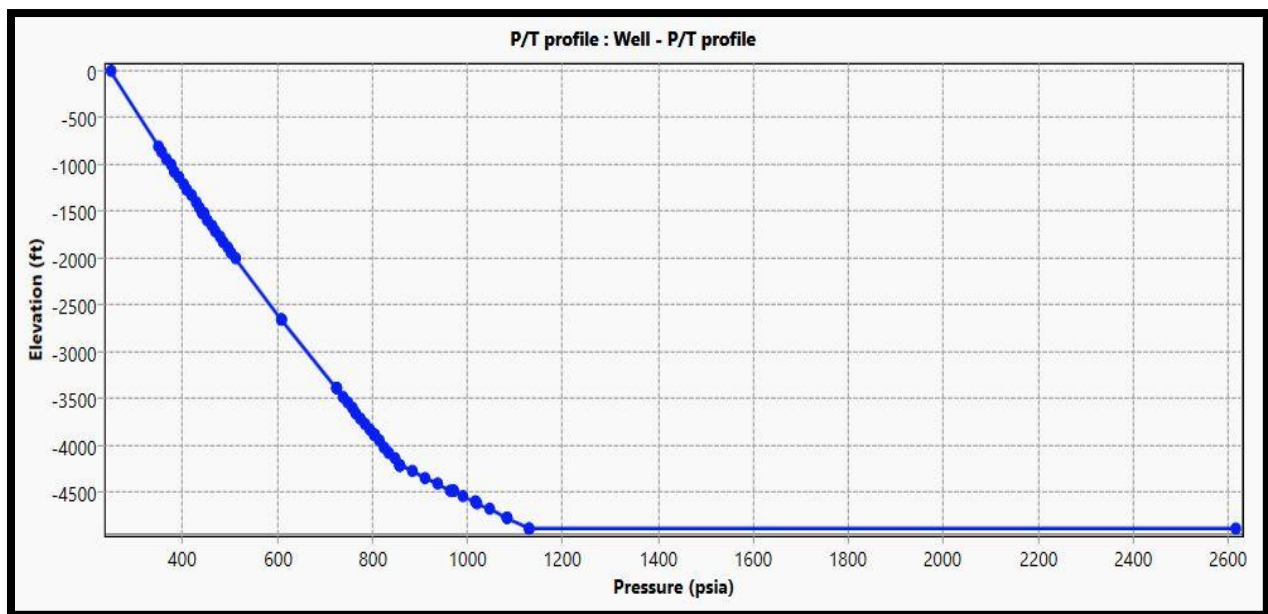


Figure 8.14 Pressure Traverse Curve after Gas Lift installation for well W31

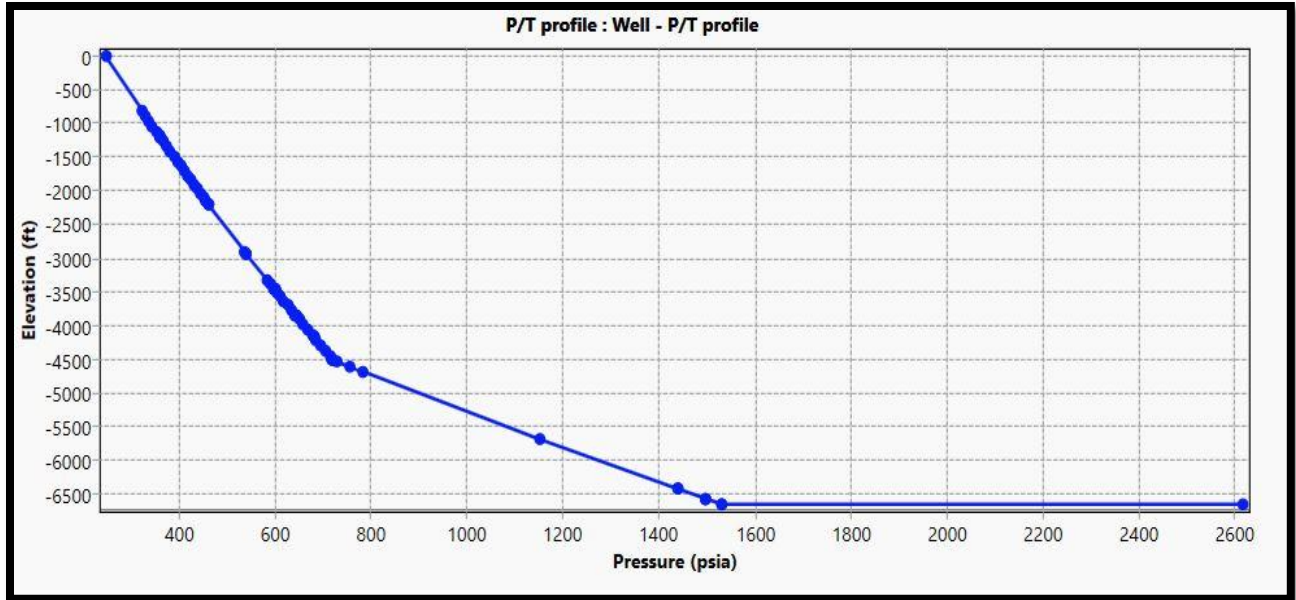


Figure 8.15 Pressure Traverse Curve after Gas Lift installation for well W33

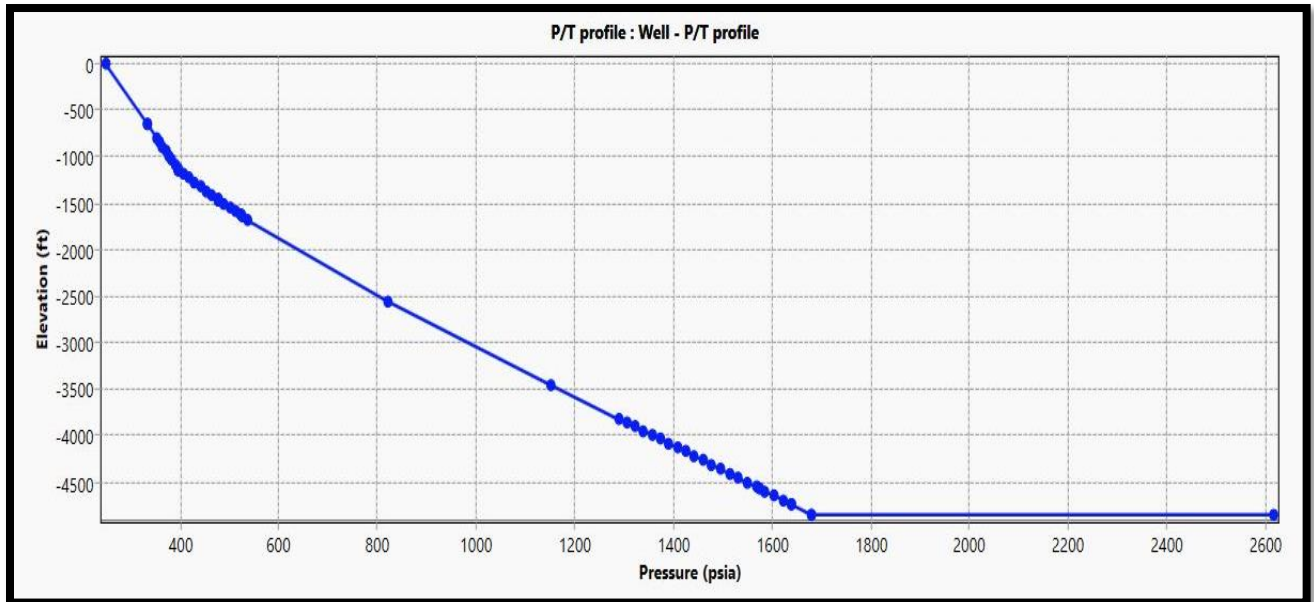


Figure 8.16 Pressure Traverse Curve after Gas Lift installation for well W48

8.APPENDIX

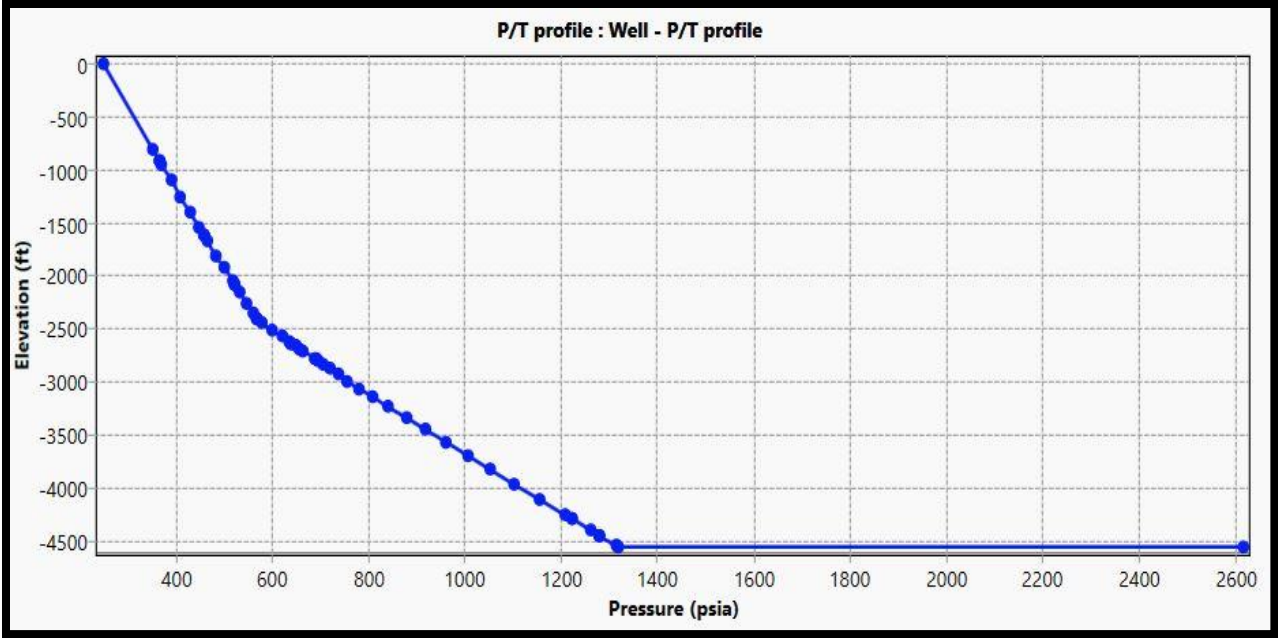


Figure 8.17 Pressure Traverse Curve after Gas Lift installation for well W50

